Theoretical and Experimental Analysis of the Possibilities of Increasing the Efficiency of the Aerosol Filtration Process in a Tangential Inlet Reverse Cyclone

Tadeusz Dziubak * and Sebastian Dziubak

Posted Date: 3 June 2026

doi: 10.20944/preprints202606.0235.v1

Keywords: air filter; main dimensions of the cyclone; filtration efficiency; flow resistance; experimental tests of the cyclone

 doi:10.20944/preprints202606.0235.v1

Article

Theoretical and Experimental Analysis of the Possibilities of Increasing the Efficiency of the Aerosol Filtration Process in a Tangential Inlet Reverse Cyclone

Tadeusz Dziubak * and Sebastian Dziubak

Faculty of Mechanical Engineering, Military University of Technology, Warsaw, Poland
* Correspondence: tadeusz.dziubak@wat.edu.pl

Abstract

A comprehensive literature review is presented regarding the influence of the cyclone inlet channel geometry and its position relative to the cyclone body, the size and shape of the outlet pipe, the configuration of the dust outlet opening to the dust collector, and the shape of the dust collector chamber on the air filtration parameters in a reverse cyclone with a tangential inlet. It was demonstrated that the outlet pipe is the cyclone element that causes the greatest pressure losses during airflow, but it also affects filtration efficiency. Modifying its design can significantly reduce the cyclone's flow resistance and, consequently, the air filter's flow resistance, which translates into lower engine power losses. To verify this hypothesis, the authors conducted a two-stage modification of the outlet pipe design of a reverse cyclone with a tangential inlet to a tracked vehicle air filter. The modification involved simplifying the inlet opening of the outlet pipe and replacing the cylindrical cyclone outlet pipe with a conical one. An experimental evaluation of the effect of these modifications on filtration efficiency and pressure drop in the cyclone was conducted. Compared to the original version, cyclone filtration efficiency has increased by 2.7% in the lower airflow range. Cyclone flow resistance has been significantly reduced, from 12 kPa to 9 kPa (20%). Reducing air filter flow resistance by 1 kPa increases engine power by 0.5-1%.

Keywords: air filter; main dimensions of the cyclone; filtration efficiency; flow resistance; experimental tests of the cyclone

1. Introduction

Every internal combustion engine draws air from the atmosphere, which is the basic component of the working medium. The mass of air inducted into the engine is proportional to the power output of the engine. In piston engines, an air flow of 1 kg/s (2800 m³/h) required for fuel combustion produces approximately 700 kW of power. The value of the air flow taken from the atmosphere by an internal combustion engine is directly proportional to the engine displacement V_{ss}, the crankshaft speed n, and the cylinder filling determined by the filling coefficient η_v. The value of η_v depends on the type of engine (naturally aspirated or supercharged), the air temperature, and therefore on the presence of an intercooler. Pressure drop in the engine intake system has a significant impact on engine filling, especially the pressure drops across the air filter, which increases systematically during vehicle use as a result of dust accumulating on the filter bed [1]. An excessive increase in air-filter pressure drop causes significant energy losses in the engine, resulting in a decrease in engine filling and power, an increase in specific fuel consumption [2,3], and an increase in exhaust smoke [4,5].

 doi:10.20944/preprints202606.0235.v1

According to the research results presented in [2], an increase in the air filter pressure drop from 2.3 kPa to 6 kPa and further to Δp_f= 12 kPa causes the filling of the cylinders in a naturally aspirated CI engine to decrease, and the curve $\eta_\upsilon = f(n)$ shifts parallel toward lower values of η_υ. At the maximum power engine speed n = 2800 rpm, the filling coefficient takes the following values: η_υ = 0.785, 0.695, 0.583. When the airflow resistance of the air filter increases by 1 kPa, the average decrease in engine air intake is 2.65%, the decrease in effective power is 0.739%, and the increase in fuel consumption remains at 0.876%.

Reference [3] reports experimental studies of the effect of air filter pressure drop Δp_f on the filling coefficient η_υ and exhaust smoke of a turbocharged engine with a classic injection system. As the air filter pressure drop increases from Δp_{f0} = 3.1 kPa (filter with a clean paper cartridge) to Δp_f = 11 kPa, 18.7 kPa, and 24.7 kPa, the filling ratio decreases to $\eta_\upsilon \approx$ 0.90, 0.81, and 0.75. An increase in resistance Δp_f by 1 kPa causes a decrease in the filling degree of an average of 1.49%, 1.29%, 1.23%. An eightfold increase in filter resistance Δp_f above the initial resistance value Δp_{f0} causes a twofold increase in engine exhaust smoke with CI.

The tests of an engine with direct fuel injection and electronic control presented in [4] showed that an increase in the pressure drop in the air filter from Δp_f = 0.580 kPa (clean filter cartridge) to Δp_{f2} = 0.604 kPa, Δp_{f3} = 0.757 kPa, and then to Δp_f = 2.024 kPa causes the filling characteristics $\eta_\upsilon = f(n)$ to shift almost parallel towards lower values. An increase in the pressure drop in the air filter from Δp_f = 0.580 kPa to Δp_f = 2.024 kPa causes a decrease in the maximum filling coefficient value from η_υ = 2.5 to η_υ = 2.39, i.e. by 4.5%. The decrease in engine power resulting from increased airflow resistance in the air filter is becoming increasingly significant: 0.029%, and 2.31%, and 9.31%; the increase in fuel consumption is: 0.39%, 1.74%, and 2.52%. However, the increase in air filter pressure drop does not cause significant changes in the degree of exhaust smoke in relation to its permissible value, specified in the technical conditions for the approval of vehicles for this type of vehicle at k = 1.5 m-1.

The air intake flow rate for car engines is 150–400 m³/h, whereas in higher-powered engines, such as those in trucks, the intake air flow is higher, ranging from 900 to 2,000 m³/h, and in engines for special-purpose vehicles (tracked military vehicles), the intake air flow is between 3,500 and 6,000 m³/h. The air demand of the turbine engine that powers the Abrams special vehicle is 5.26 kg/s (16,000 m³/h) [6].

The atmosphere contains various solid, gaseous, chemical, and biological pollutants that are emitted into the atmosphere by natural and artificial sources. Solid particles that pollute the air fall to the ground under the influence of gravity. In this way, significant amounts of industrial dust, volcanic dust, or dust from desert regions, which are transported over long distances, fall onto the road surface. Mineral dust also settles on road surfaces, carried by the wind from areas adjacent to the road, such as farmland, residential construction sites, and generated during road repair work.

Recent years have shown that a very important problem related to air pollution is the emission of automotive pollutants other than exhaust gases, known as “non-engine emissions.” This is the phenomenon of emissions into the environment of dust from the wear of clutch friction linings [7] and brake pads and brake discs of cars [8–10], as well as tires and road surfaces [11–13]. As stated by the authors of the study [14], road dust contains a large number of different chemical elements. The highest concentrations were found for Ca, Si, and Al, at 373.3 mg/g, 351.4 mg/g, and 113.9 mg/g, respectively. The presence of K, S, Cd, Sb, Pb, Ni, and Zn was also detected in the dust.

Heavy metals in road dust are mainly found in particles originating from worn vehicle components, such as tire treads, brake pads, and brake discs. Heavy metals are also found in abrasive wear products from piston-piston ring-cylinder liner (P-PR-CL) assemblies and are emitted along with exhaust gases from tailpipes [15].

Solid pollutants lying on roads can be dispersed and re-suspended in the atmosphere as a result of turbulence caused by motor vehicle traffic or gusts of wind, hence they are commonly referred to as “road dust” [14]. Road dust is a general term for any form of particulate matter (PM) that settles on the road surface. Road dust contains significant amounts of mineral dust. The highest concentrations of mineral dust are suspended in the air when vehicles travel on dry, unpaved terrain,

 doi:10.20944/preprints202606.0235.v1

as well as when helicopters are used in situations where makeshift landing sites are necessary. Dust is characterized by the following properties: chemical composition, grain composition (polydispersity), morphology, grain size, settling velocity, grain density, angle of repose, specific surface area, porosity, wettability, specific resistance, toxic, flammable, and explosive properties. Knowledge of the properties of dust is essential to assess the hazards associated with it, evaluate its behavior in the air, and select a method for removing it from contaminated gases.

The impact of dust on the structural parts of internal combustion engines (turbine and piston) requires knowledge of the properties of dust, which are characterized by the following parameters: concentration in the air, chemical composition, hardness, fractional (granulometric) composition, density, grain shape, and tendency to coagulate.

The percentage content of individual components in particulate matter is determined by its chemical composition, and its main component is SiO_2, which accounts for 60–95% of the particulate matter. The remainder consists of oxide-based components: aluminum oxide (corundum, Al_2O_3), iron oxides, calcium oxides, and magnesium oxides. In smaller quantities, not exceeding 3%, the dust may contain other oxides, such as SO_2, K_2O, Na_2O, NiO_2, and TiO_2 [16–18]. Furthermore, the chemical composition and physical properties of dust depend on the geographical location, type of road and soil, vehicle traffic intensity and other local conditions, weather and environmental conditions (wind, rain, snow, frost, drought), vehicle design, and the location and design of the air intake system, as well as the height of the intake above ground level. Climatic factors (wind, rainfall, snowfall, frost, drought) and atmospheric fallout of industrial dust, forest fire dust, and volcanic dust have a significant impact on the chemical composition [19].

The hardness, density, and shape of dust particles depend on their chemical composition. Silica has a hardness of 7, and corundum has a hardness of 9 on the Mohs scale. These materials account for up to 95% of the dust. The hardness of structural materials used in the construction of modern engines is significantly lower than that of dust particles, which take the form of irregular solids with sharp edges, similar in shape to polyhedrons. For this reason, determining their sizes presents significant difficulties. For this reason, the concept of equivalent diameter, denoted by d_p, is used to assess particle dimensions.

Road dust is polydisperse, meaning it contains particles of varying sizes. This property of the dust is defined by its particle size distribution, which depends on the type of road surface and the height above the surface, due to the different settling velocities of the particles in the air. For example, silica particles (density 2650 kg/m³) with sizes of 10 and 100 μm settle at speeds υ_d = 0.035 and 0.72 m/s [20]. In contrast, for particles with a density of 1000 kg/m³ and diameters of 0.1 μm and 1 μm, υ_d is 4×10^{-7} m/s and 4×10^{-5} m/s, respectively [21,22]. Particles with a size of 10 μm fall in still air at a velocity $\upsilon_d = 3 \times 10^{-3}$ m/s, which is significantly lower than that of dust particles with a diameter d_p = 100 μm, for which $\upsilon_d = 3 \times 10^{-1}$ m/s. This explains why dust with particle sizes d_p = 2–10 μm has a significantly longer residence time in the air, resulting in these dust particles being sucked into the engines along with the air [4].

The concentration of dust in the air is a measure of the mass of dust (in grams or milligrams) in 1 m³ of atmospheric air. Reported airborne dust concentrations vary widely depending on road type, vehicle operation, terrain, and environmental conditions. For this reason, the values of dust concentration in the air for different conditions of use of vehicles and working machines and different surfaces vary widely [23–33].

The authors of [23,24] report that dust concentration in the air can reach values ranging from 0.139 to 57 mg/m³ on paved roads and up to 3000 mg/m³ during severe sandstorms.

According to the authors [24,25], airborne dust levels in residential areas range from 0.010 to 0.139 mg/m³, from 30 to 8000 mg/m³ when a convoy of vehicles is traveling on a dirt road, and from 1000 to 10,000 mg/m³ during a sandstorm. Research presented in [27] shows that at a distance of several meters behind a tracked vehicle traveling at speeds of 10 and 30 km/h on dry, sandy ground, airborne dust levels reached a maximum value of 480 and 1170 mg/m³, respectively. The authors of [28] report that the average airborne dust levels in the air at the height of the upper armor of a tracked

 doi:10.20944/preprints202606.0235.v1

vehicle traveling at a speed of 14-18 km/h on sandy terrain is 1500-2900 mg/m³ and reaches a maximum value of 3800 mg/m³ in the stern of the vehicle. When driving at higher speeds, the dust concentration increases and reaches 7000 mg/m³ in the stern of the vehicle. Driving wheeled vehicles in a convoy with small gaps on sandy terrain causes dust concentrations in the air to exceed 2000 mg/m³, while a single vehicle driving on unpaved roads generates concentrations of 10-30 mg/m³ [30]. During the takeoff or landing of a helicopter on an emergency landing site at the height of the CH-53 helicopter propeller (0.5 m above ground), the airborne dust levels reached a value of approximately 3330 mg/m³ [31,32]. According to the authors of [33], at a airborne dust levels of 600-700 mg/m³, visibility is reduced, and when the value exceeds 1500 mg/m³, visibility becomes zero.

Engines in vehicles operating in environments with high dust concentrations draw significant amounts of dust into their cylinders. For example, a tracked vehicle engine with a displacement of V_{ss} = 38.8 dm³, traveling over sandy terrain at a dust concentration of s = 1 g/m³, can draw in nearly 200 kg of dust along with the air over 50 hours of operation, which amounts to approximately 0.06 kg per minute. In contrast, a helicopter whose engine has an air demand of 5.9 kg/s draws in over 0.7 kg of dust per minute [34] at a dust concentration in the air of 2.5 g/m³.

Mineral dust particles enter the headspace of the engine cylinders, where approximately 10–20% adhere to the oil film on the cylinder liner wall. The dust particles mixed with oil form an "abrasive paste" that penetrates the gaps between the piston and cylinder as well as the piston rings, contributing to accelerated abrasive wear of these components. In mineral dust, the main components (approximately 70–90%) are hard silica grains (7 on the Mohs scale) and corundum (9 on the Mohs scale). Furthermore, the grains of these minerals have irregular shapes and sharp edges, which results in accelerated abrasive wear upon contact with engine components. The P-PR-C assembly (piston-piston rings-cylinder wall) is particularly sensitive to mineral contaminants. Typically, the oil film thickness in engine assemblies ranges from 0.1 to 50 μm [35]. In modern engines, this film is significantly thinner, ranging from 0 to 10 μm [36]. All dust particles whose size at a given moment equals the thickness of the oil film cause abrasive wear. It follows from the above that all dust particles larger than the minimum oil film thickness (0.1 μm) should be removed from the air stream [37], which is the task of the air filter.

When the piston is at the top of the cylinder bore during the power stroke, the conditions for the formation of an oil film are particularly difficult. This is due to a decrease in oil viscosity caused by the high temperature of the exhaust gases and the piston. The authors of [24,38–40] state that abrasive wear of internal combustion engine components is caused mainly by mineral dust particles ranging in size from 1 to 40 μm. However, the greatest wear results from the interaction with dust particles ranging in size from 1 to 20 μm.

Excessive wear of the P-PR-C system components results in excessive clearance, which causes increased loss of fresh charge, which leaks into the engine crankcase, resulting in a drop in compression pressure and, consequently, a drop in engine power. The resulting leaks in the P-PR-C assembly cause increased exhaust gas flow into the engine crankcase. This causes an increase in oil temperature and a decrease in its viscosity, which can cause oil film breakdown and increased friction losses in the piston-ring-cylinder configuration [41,42]. Soot in the exhaust gases accumulates in the oil, accelerating its aging [43,44].

In order to ensure the appropriate purity of the intake air for combustion engines of motor vehicles and work machines, two-stage air filters are used in the engine intake systems, where the first stage of filtration is an inertial filter (multi-cyclone), and the second stage of air filtration is a filter insert made of pleated filter paper or other filter material arranged in series behind it. The essence of filtration in a two-stage filter is that the multicyclone retains a significant amount of mineral dust with moderate efficiency (87-95%) and for particles larger than 15-35 μm and directing the remaining (insignificant) mass of dust to a paper filter, where it is separated with an accuracy of over 99.5% and an accuracy above 2-5 μm. Thus, the increase in pressure drop of the porous barrier is less intense, which extends the period of efficient operation of the system until the permissible pressure drop value is reached.

 doi:10.20944/preprints202606.0235.v1

Multicyclones suitable for filtering engine intake air consist of tens to hundreds of cyclones arranged parallel to each other, most often with internal diameters not exceeding D = 40 mm. The filter elements of a multicyclone can be reverse cyclones with a tangential or axial inlet and straight-through cyclones with an axial inlet (Figure 1). Conventionally designed tangential inlet reverse cyclones used in motor vehicles are characterized by up to 95% efficiency in filtering mineral dust containing particles smaller than 80 μm, but with low (above 35 μm) accuracy and significant (2-2.5 kPa) pressure drop [26,45–48]. Under the same air filtration conditions, axial inlet cyclones are characterized by lower pressure drop but achieve lower filtration efficiency in the range of 80-87% [49–52].

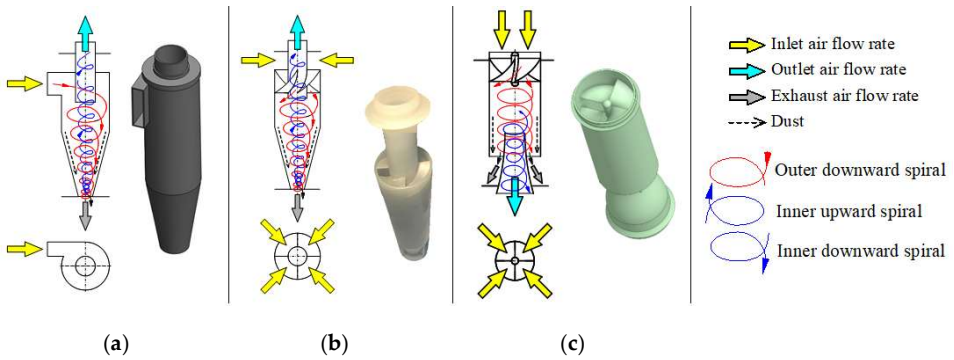

Figure 1. Types of cyclones for air filters: (**a**) tangential return cyclone, (**b**) axial return cyclone, (**c**) axial through-flow cyclone [52].

Figure 2 shows the author's comparative analysis of the filtration efficiency characteristics $\varphi_c = f(Q_G)$ and pressure drop characteristics $\Delta p_c = f(Q_G)$ of three reverse cyclones (A, B, C) and two axial inlet cyclones (D, E). At a maximum inlet velocity of υ_{0max} = 60 m/s (corresponding to an air flow rate through a single cyclone of Q_G = 30 m³/h), cyclone A achieves a pressure drop of 12 kPa, which is several times higher than the pressure drop of other types of cyclones. At the same air flow rate, the pressure drop of cyclone B does not exceed 2.5 kPa, while the resistance of cyclones D and E is 0.36 kPa and 0.58 kPa, respectively. The filtration efficiency of cyclones (A, B, C, D, E) varies significantly and for Q_G = 30 m³/h, they take the following values: 96.9%, 95.6%, 91%, 87.7%, and 85.2%, respectively. The above analysis shows a close relationship between filtration efficiency and cyclone flow resistance, indicating that the greater the flow resistance, the greater the efficiency, and vice versa.

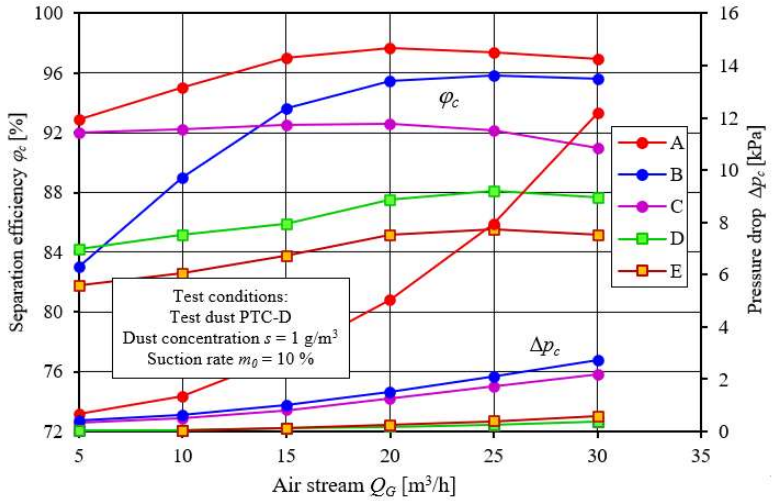

Figure 2. Filtration efficiency $\varphi_c = f(Q_G)$, flow resistance $\Delta p_f = f(Q_G)$ of cyclone air filters in special vehicles [52].

 doi:10.20944/preprints202606.0235.v1

The durability of internal combustion engines, particularly those in off-road vehicles and special-purpose vehicles that operate in environments with high levels of airborne dust, require air filters with high efficiency, low flow resistance, and high filtration precision. These requirements are met by two-stage air filters, where the first stage of filtration consists of a cyclone bank. The use of cyclones with high filtration efficiency reduces the amount of dust directed to the second filtration stage, resulting in a slower increase in flow resistance and, consequently, extending the interval between filter element replacements. Measures to reduce the flow resistance of the cyclones are also essential, as this will positively impact engine power.

When it comes to cyclone dust collectors, the two most important factors to consider are flow resistance and filtration efficiency, where flow resistance represents the energy required to operate the cyclone and separation efficiency represents the efficiency of the device. In practical applications, a higher flow resistance results in increased energy consumption and a decrease in engine power. Therefore, in order for the cyclone design to be balanced and economical, the pressure drop must be evaluated together with the separation efficiency.

The analysis shows that the main pollutant in the air ingested by vehicle and machinery engines is hard mineral dust particles, which, once they enter the engine's friction areas, cause accelerated wear of engine components. As a result, the clearance between the interacting components (for example, in a P-PR-LC circuit)) increases, which leads to a decrease in engine power and increased emissions of harmful exhaust components. This phenomenon of accelerated wear is effectively counteracted by two-stage air filters, where the first stage is a set of reverse cyclones with a tangential inlet or through-flow cyclones with an axial inlet.

There are two approaches in this regard: increasing the filtration efficiency of cyclones, which will reduce the amount of dust directed to the second stage of filtration (partition filter), thus extending the vehicle's service interval and reducing pressure drop in the intake system, thereby minimizing the drop in engine power. These measures are contradictory, as increasing efficiency is associated with an increase in pressure drop and, conversely, lower efficiency means lower pressure drop.

The efficiency of gas filtration in a cyclone and the resulting pressure drop within the cyclone depend on numerous geometric parameters of the device, as well as on the airflow and dust conditions inside it; hence the need to understand how these factors affect the cyclone's operating parameters. This will allow for the design of a cyclone with optimal parameters. There is a significant number of studies in this field in the available literature, and their review, systematization, and appropriate analysis will allow for the creation of a knowledge base in this area, which is the objective of the present study. This information can be used in the design and optimization of cyclones.

Section 2 reviews, the authors presented a literature review on the potential for improving filtration efficiency in a tangential-inlet reverse cyclone by modifying selected design elements, without altering the cyclone's main dimensions. In the manuscript, the authors focused on four areas where such modifications are possible, namely: modifying the geometry of the cyclone inlet duct and the shape of the cyclone outlet tube; changing the configuration of the outlet opening; and altering the shape of the cyclone body. The use of original (unconventional) cyclone design solutions and the benefits thereof were also analyzed.

In the third main chapter of this thesis, to corroborate the findings of the literature review, the authors present the results of their own experimental studies on modifications to the outlet tube of a return cyclone. The cyclone under study is a component of a multicyclone that serves as an air filter for a tracked vehicle. Experimental studies of two modifications of this cyclone demonstrated an improvement in its efficiency in terms of filtration effectiveness and flow resistance.

 doi:10.20944/preprints202606.0235.v1

2. Analysis of Opportunities to Improve Filtration Efficiency in a Tangential Reversing Cyclone

A cyclone separator is a typical device that uses centrifugal force to separate gases and solids. Due to its advantages of simple design, high operational flexibility, high efficiency, and minimal servicing and maintenance, it is widely used for dust removal from industrial exhaust gases and for filtering the intake air of vehicle engines operating in dusty environments.

The geometric parameters, determined by the cyclone's design dimensions, as well as the gas flow parameters (inlet velocity υ_0, temperature, viscosity, and density) and dust parameters (chemical and fractional composition, particle density, and shape) determine the cyclone's performance [53]. The condition for achieving high filtration efficiency and low-pressure losses in the cyclone is maintaining the appropriate proportions of the design dimensions of each of its parts.

For inverted cyclones with a tangential inlet, these proportions-expressed as the ratios of their principal dimensions-have been determined through many years of research and presented in [54–63]. The research indicates a mutual relationship between the cyclone's main dimensions. The results of the research allowed for the determination of such ratios in the form of quotients of the two principal components, for which the cyclone achieves optimal operating conditions, taking maximum separation efficiency and minimum pressured drop as criteria. The paper [63] presents examples of the ratios of the main dimensions (Figure 3) of tangential inlet return cyclones as reported by various researchers (Table 1).

Table 1. Ratios of the main dimensions of various types of tangential inlet return cyclones.

Cyclone parameter	High efficiency		Conventional		High Throughput	
	Stairmand 1951	Swift 1969	Lapple 1951	Swift 1969	Stairmand 1951	Swift 1969
Body diameter D/D	1.0	1.0	1.0	1.0	1.0	1.0
Heigth of inlet a/D	0.5	0.44	0.5	0.5	0.75	0.8
Width of inlet b/D	0.2	0.21	0.25	0.25	0.375	0.35
Diameter of gas exit d_w/D	0.5	0.4	0.5	0.5	0.75	0.75
Length of vortex Finder h/D	0.5	0.5	0.625	0.6	0.875	0.85
Length of Body H_c/D	1.5	1.4	2.0	1.75	1.5	1.7
Length of cone H_s/D	2.5	2.5	2.0	2.0	2.5	2.0
Diameter of dust outlet d_e/D	0.375	0.4	0.25	0.4	0.375	0.4

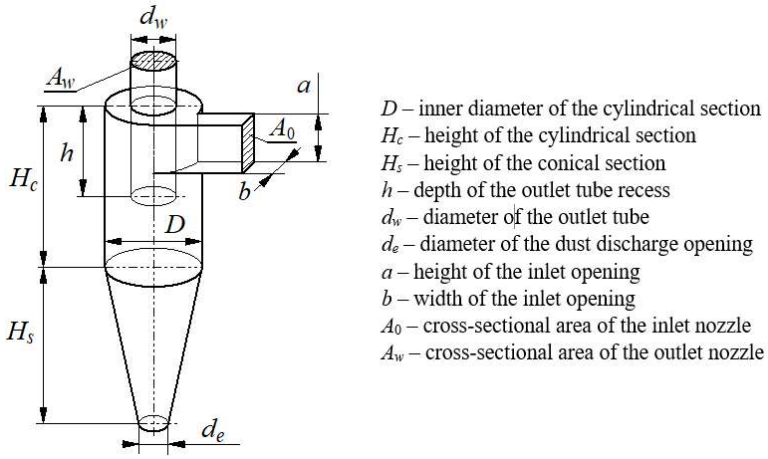

Figure 3. Basic dimensions of a tangential inlet return cyclone.

 doi:10.20944/preprints202606.0235.v1

The examples shown (Figure 4) of changes in separation efficiency φ_c and pressure drop coefficient ξ_c depending on the coefficients A_w/A_0 and H/d_w demonstrate that the optimal range of these parameters lies between 1.5–2 and 7–9 [54]. The relationship for the coefficient ξ_c is given by the formula:

$$\xi_c = \frac{2\Delta p_c}{\rho_p \cdot \upsilon_w^2}, \quad (1)$$

where: ρ_g – gas density, Δp_c – gas pressure drops through the cyclone, υ_w – cyclone outlet velocity.

Using this data during cyclone design allows for relatively high filtration efficiency of intake air for combustion engines with respect to micro-sized particles.

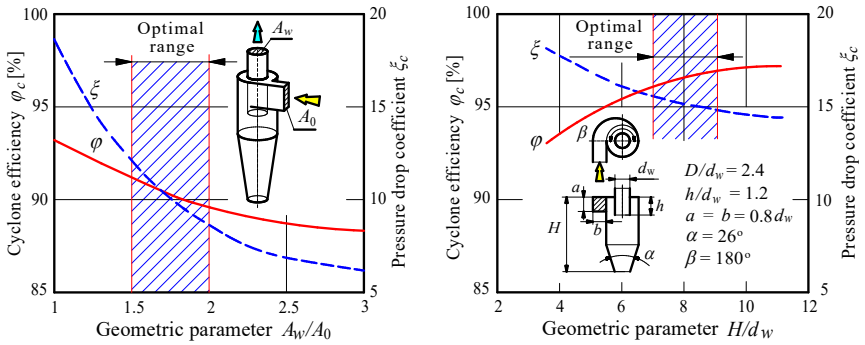

(**a**) (**b**)

Figure 4. Cyclone efficiency φ_c and coefficient ξ_c as a function of (**a**) the parameter A_w/A_0, (***b***) the parameter H/d_w. The figure was created by the authors using data from [54].

The scientific literature indicates that research is ongoing to improve the efficiency of particulate separation in cyclones and to reduce aerosol flow resistance within the cyclone by modifying the design of selected cyclone components within the existing main geometric dimensions. The research results presented in the literature demonstrate that numerous studies of tangential-inlet reverse-flow cyclones have been conducted in this area, including both experimental and numerical studies. These studies focus on individually assessing the impact of specific geometric parameters of the cyclone on its fundamental characteristics: filtration efficiency and flow resistance.

Most studies on this topic have focused on improving cyclone efficiency compared to baseline models based on geometric parameters, including inlet geometry [64–92], changes in the configuration of the cylindrical and conical parts of the cyclone [92–95], the size and shape of the outlet pipe [96–109], the configuration of the lower opening of the conical part of the cyclone and the shape of the dust collector [110–116], the use of additional elements inside cyclone separators, or the use of original (unconventional) cyclone design solutions [117–120].

2.1. Modification of the Cyclone Design by Changing the Geometry of the Inlet Duct and Its Position Relative to the Cyclone Body

Research on cyclone geometry involved modifying the cyclone inlet duct, which results in a change in the airflow path leading to the main (cylindrical) section of the cyclone. Since the tangential aerosol inlet duct determines how air and particles enter the cylinder body, its design has a significant impact on the cyclone's filtration characteristics, which requires designers to design it appropriately.

Cyclone geometry determines the inlet velocity and its distribution. In general, both filtration efficiency and flow resistance increase as the velocity of the gas and particles at the inlet increases [64–69], which means that filtration efficiency increases as the cross-sectional area of the inlet channel decreases. Rectangular inlets, which are commonly used in industry and automotive applications, have higher filtration efficiency than circular and elliptical inlets [70,71]. Appropriately reducing the inlet duct width and height effectively improves filtration efficiency [72–74].

 doi:10.20944/preprints202606.0235.v1

The study [70] examined the influence of cyclone geometry using symmetrical double and quadruple inlets and different cross-sections (rectangular, circular, and elliptical) of the inlet channel. It was found that a cyclone equipped with a double inlet exhibits a filtration efficiency that is 20-25% higher than that of a cyclone with the same geometry but a single inlet. The use of four inlet channels to the cylindrical section of the cyclone increases its filtration efficiency by 40-45%, while the total cross-sectional area of two and four inlet channels and a single channel have the same value as.

It was also found that a cyclone with a rectangular inlet has a filtration efficiency that is 4-6% higher than that of a cyclone with an elliptical inlet. It was also demonstrated that the filtration efficiency of a cyclone with an elliptical cross-section inlet duct is 30-35% higher than that of a cyclone with a circular cross-section inlet.

The authors of [71] conducted research on the impact of changing the shape of the inlet duct (cross-section) to the cyclone on air flow and flow resistance, as well as the value of the cut-off particle size in cyclones with multiple inlets. They tested five inlet geometries, including a circle, an ellipse, a square, a rectangle, and a trapezoid. It was found that cyclones with rectangular inlets had significantly higher tangential velocities, while circular and square inlet ducts resulted in the lowest pressure drop.

In [73], the effect of the dimensions of a rectangular cyclone inlet (*b*-width and *a*-height) on filtration efficiency and pressure drop was analyzed. It was found in the five cyclones studied that increasing the width "b" or height "*a*" of the rectangular cyclone inlet results in a reduction in flow resistance but has a negative effect (increase) on the d_{p50} size of the separated particles. It was demonstrated that changes in the width "*b*" have a more significant effect on the d_{p50} diameter than changes in the height "*a*." It was determined that the most favorable b/a ratio should be in the range of 0.5-0.7.

The inlet duct for a reverse cyclone with a tangential inlet determines the mass distribution of dust particles across its cross-section. The authors of [75–81] demonstrated that using an asymmetric inlet with a curvilinear lateral plane instead of a symmetrical rectangular inlet and an inlet oblique to the cyclone's main axis of symmetry [82–84] results in a more favorable mass distribution of dust particles in the inlet port cross-section and directs a significant amount of dust (already in the inlet) toward the inner wall of the cyclone's cylindrical body, which significantly facilitates and accelerates the separation of solid dust particles from the air and results in increased separation efficiency. Using a banded inlet on the cylindrical part of the cyclone results in a gentler mixing of the inlet stream with the stream already rotating in the cyclone, which can reduce pressure drop [85,86]. Previous studies have shown that having more than one aerosol inlet pipe to the cyclone and installing them symmetrically (at equal intervals on the same level) around the circumference of the cylindrical section results in a significant increase in filtration efficiency and a reduction in flow resistance [87–91].

Reference [67] presents several methods for directing an air stream into the cylindrical section of a return cyclone (Figure 5) in order to induce strong swirling in the form of a tangential velocity component with a high value. The most used configurations feature tangential (spiral) air supply. The spiral inlet is designed to cover the cylindrical section over 180 arcs. Configurations with an axial inlet in the form of deflectors (usually 4) inclined at an angle are also used.

 doi:10.20944/preprints202606.0235.v1

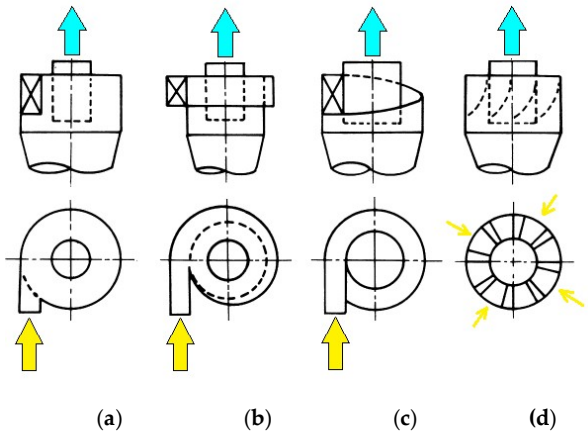

Figure 5. Schematic diagrams of air flow into a reverse cyclone housing: (**a**) tangential flow inlet, (**b**, **c**) tangential flow inlet with a spiral inlet, (**d**) axial flow inlet. Figure prepared by the authors using data from [67].

The paper [82] presents the results of numerical studies of cyclones aimed at evaluating the effects of changes in the angle of the inlet duct with a rectangular inlet on flow resistance and flow structure. Five cyclones with spiral inlets and various inlet angles were numerically analyzed, as well as another five cyclones with tangential inlets but with different heights of the rectangular inlet, while keeping the remaining geometric dimensions unchanged (Figure 6).

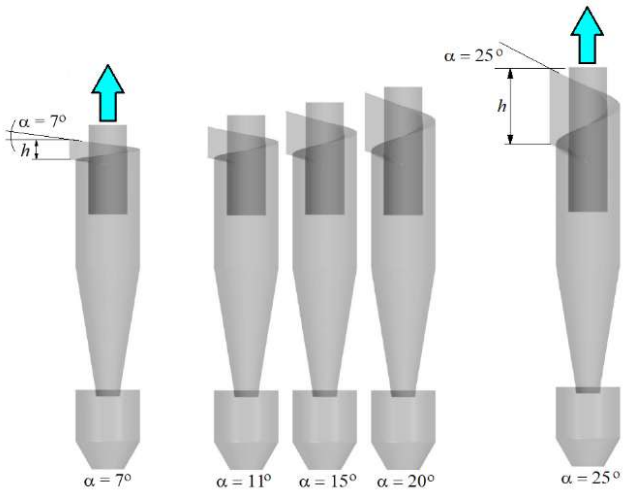

Figure 6. Cyclones with spiral roof inlets of various angles of inclination and inlet heights. Figure created by the authors using data from [82].

Increasing the angle and height of the rectangular inlet (cross-sectional area) results in a decrease in pressure and tangential velocity within the cylindrical section of the cyclone, which significantly reduces filtration efficiency. Increasing the inlet angle of the duct reduces the gas flow along the cyclone's main axis, regardless of whether it is an external spiral (downward) or internal vortex (upward) motion. There is also an increase in the maximum radial velocity at the inlet to the outlet tube. In this way, the number of small dust particles entrained by the internal upward-spiraling gas stream may increase. This negatively affects the filtration efficiency in the cyclone. In contrast, flow resistance in the cyclone decreases significantly as the inlet angle of the inlet duct increases. Cyclones with tangential inlets have lower separation efficiency than cyclones with an angled inlet duct, and these cyclones achieve their highest aerodynamic efficiency when the inlet angle is 20°.

The article [83] presents a study on the effect of the angle of inclination of the aerosol inlet pipe with a rectangular cross-section relative to the main axis of symmetry of the cylindrical part of the

 doi:10.20944/preprints202606.0235.v1

reverse cyclone on its filtration efficiency and pressure drop. The angular inclination (α = −30°, −15°, 0°) of the inlet pipe downwards relative to the horizontal and the upward inclination (α = 0°, 15°, 30°) were examined. The results indicate that the angle of inclination of the inlet pipe causes a change in the direction of gas introduction, which results in changes in flow resistance and separation efficiency.

As the inclination angle α of the aerosol inlet duct changes from (α = -30°), the flow resistance decreases and for α = 0° (horizontal inlet position), it reaches a minimum value (1118 Pa) and then increases with increasing inlet duct angle, reaching a value of 1145 Pa at a positive angle α = 30°. The results indicate that a negative inlet duct angle causes greater flow resistance than positive inlet angles of the same value. As the inlet angle increases, the filtration efficiency systematically increases and reaches a maximum value at a positive angle (15°) and then decreases. From the above, it can be seen that the optimal operating range of the cyclone appears to be in the range from -15° to 15° of inlet duct angle.

The study [84] analyzed the effect of the inlet duct bend angle on filtration efficiency and pressure drop in an inverted cyclone compared to cyclones with tangential inlets. Twenty cyclones with different inlet duct bend angles for the air stream were examined. Ten inlet duct bend angles in the vertical plane and ten angles in the horizontal plane were tested (in the range of a = -90° to 90°). The data obtained indicate that the bending angle (in the vertical and horizontal planes) does not have a significant effect (maximum difference of 3.1%) on filtration efficiency. All comparisons were made with reference to the baseline variant at α = 0° and β = 0°.

The authors of [86] investigated the effect of inlet spiral wrap angle on double-inlet cyclone separators using CFD. The results indicated that spiral wrap angles of 0° and 90° improved collection efficiency for particles below 10 μm in diameter, while 180° provided no benefit. For optimal performance, the appropriate wrap angle must be selected, as it significantly affects tangential velocity and overall cyclone efficiency.

In [91], a study was presented of the influence of the radial angle (angle between adjacent inlet channels) of five identical inlet channels to a reverse cyclone with tangential inlet on its filtration efficiency. The studies were carried out at inlet velocities in the range of 2-6 m/s for the following radial angles of the inlet channel: θ = 15°, 32°, 45°, 61° and 72°.

If the cyclone inlet velocity is υ_0 = 6 m/s, the maximum flow resistance (84.5 Pa) occurs at an inlet radial angle θ = 15°, while the minimum flow resistance (77.42 Pa) occurs at an angle θ = 32°. The filtration efficiency varies depending on the inlet angle θ. With increasing channel inlet angles θ = 32°, 45°, 15°, 72° and 61°, the filtration efficiency reached increasingly higher values of 89.0%, 91.7%, 92.5%, 94.7% and 94.8%, respectively. At the same time, it was found that the boundary grain diameter decreased, ranging from d_{50} = 1.17 μm to 1.38 μm.

More new modifications to the tangential inlet configuration of the reverse cyclone and their impact on its operating efficiency can be found in [53,92].

The effect of different height variants of the conical and cylindrical parts on the efficiency of cyclones with tangential inlets was presented in [93]. Three different variants of the relationship H/D = 0.5, 1.0, and 1.5 were tested, where D = 0.205 m is the cyclone body diameter. Three different variants of the cyclone conical part profiles were also analyzed: straight profile (ST), convex profile (CV), and concave profile (CC). For three different cyclone inlet velocities: υ_0 = 10 m/s, 15 m/s, and 20 m/s, the characteristics of filtration efficiency and flow resistance were determined. The test results show that with increasing height of the cylindrical part of the cyclone, flow resistance decreases in all tested cyclone variants, while filtration efficiency slightly decreases. Additionally, it was observed that the d_{50} cut-off value slightly increased.

2.2. Modification of the Cyclone Design in Terms of the Shape of the Outlet Tube

The analysis of the results of previous studies confirms that the energy losses caused by the air flow through the cyclone outlet tube (vortex finder) constitute a very large (about 70%) share of the

 doi:10.20944/preprints202606.0235.v1

total gas pressure losses in the cyclone [96–106]. As the outgoing gas stream continues to swirl in the outlet tube, a pressure loss occurs, which depends on the cyclone geometry and can reach up to 50% of the total pressure drop in the cyclone [96]. There are many options for reducing pressure drop through this element. Streamlining the inlet opening of the traditional cylindrical outlet tube [97] and replacing the cylindrical tube with a conical one while maintaining the outlet tube inlet diameter d_w can significantly reduce pressure drop in the cyclone without reducing filtration efficiency [98–101]. Another method of reducing flow resistance in a reverse cyclone with tangential air supply is the use of special guide vanes (deswirlers) inside the gas outlet tube from the cyclone, whose task is to convert the spiral motion of the gas stream inside the outlet tube into a rectilinear motion [102,103]. Special tips (deswirlers) can also be used at the outlet tube inlet, which straighten the swirling stream and convert the kinetic energy into static pressure [103]. Alternatively, a special detector (slotted vortex finder) can be used to improve the filtration efficiency of the cyclone separator, including reducing the pressure drop [104,105].

Reference [96] describes ways to shape the inner tube of a cyclone, which allows for a reduction in pressure drop within the cyclone by using a cylindrical tube with a streamlined inlet opening, a conical tube, and a tube with guide vanes (Figure 7), which convert the kinetic energy of the rotational motion of the gas flowing inside the outlet tube into the kinetic energy of the linear motion of the gas stream.

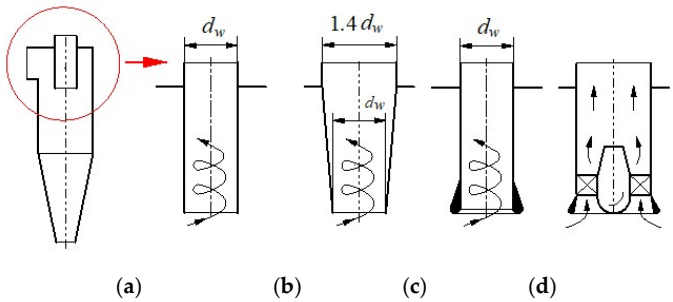

Figure 7. Possibilities of shaping the inner tube of a cyclone: (**a**) commonly used cylindrical tube, (**b**) tube with an inverted cone, (**c**) cylindrical tube with a streamlined inlet, (**d**) tube with guide vanes at the inlet. Drawing prepared by the authors using data from [96].

In [98] experimental studies of the influence of two types of outlet pipes (vortex) on the filtration efficiency and flow resistance of a reverse cyclone with a single and double tangential inlet were presented. Four cyclone variants were tested:

Type 1A – cyclone with a single inlet and a cylindrical outlet pipe

Type 1B – cyclone with a single inlet and an inverted conical outlet tube (the inlet opening has a smaller diameter)

Type 2A – cyclone with a double inlet and a cylindrical outlet tube

Type 2B – cyclone with dual inlet and inverted conical outlet tube

It was found that increasing the diameter of the outlet tube reduces separation efficiency but also flow resistance in cyclones with two inlet channels. The results indicate that an outlet tube with an inverted conical cross-section provides higher separation efficiency, but also greater flow resistance. A cyclone with two inlet channels and a cylindrical outlet tube exhibits higher separation efficiency but also greater flow resistance.

Article [101] presents the results of studies on several variants of a return cyclone (D = 30 mm) with different outlet tube shapes of the same length but varying geometries. The cyclone was tested with cylindrical tubes of diameters d_w = = 7, 11, 15 mm, with conical tubes (converging and diverging) of cone length h_s = 10, 25, 45 mm, and with two diameters d_1 = 7 and d_2 = 15 mm at the end of the cone (Figure 8).

 doi:10.20944/preprints202606.0235.v1

The filtration efficiency of different cyclone variants was determined using monodisperse test dust (PSL) with a density of 1.05 g/cm^3 for two different air flow rates Q = 30 and Q = 50 dm^3/min. Cyclones with conical outlet tubes showed higher filtration efficiency than cyclones with a cylindrical outlet tube with a diameter of d d_w = 15 mm and lower efficiency than a cyclone with a cylindrical outlet tube with a diameter of d_w = 7 mm.

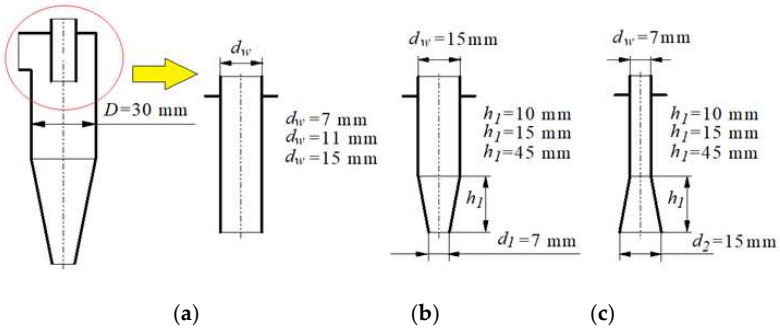

Figure 8. Shapes of cyclone outlet pipes: (a) cylindrical pipe, (b) outlet pipe with a tapered inlet, (c) outlet pipe with a flared inlet. Figure created by the authors using data from [101].

An example of the use of special guide vanes (deswirlers) inside the cyclone's gas outlet tube, whose function is to convert the spiral motion of the gas stream inside the outlet tube to rectilinear motion, is shown in [103]. Numerical studies have shown that extending the vortex detector has a negligible effect on the pressure drop and cyclone efficiency. The closer the deswirler is installed to the outlet tube inlet, the more significant its effect on cyclone efficiency. A streamlined, ellipsoidal shape of the deswirler's central body is advantageous over a cylindrical one, as it leads to lower pressure losses. Compared to a standard configuration, a deswirler with a streamlined, ellipsoidal central body reduces pressure losses by 74%. This leads to a 32% reduction in total pressure drop without compromising the cyclone's separation capacity.

In [104], a numerical analysis was conducted of four geometric parameters of the deswirler (including the number of blades, core diameter, blade height, and blade angle) in a cyclone separator. The geometry of the deswirler was examined numerically in terms of its impact on flow resistance and filtration efficiency. The deswirler converts the energy of the swirling flow in the outlet pipe into linear motion, thereby reducing flow resistance by 95.67%, which results in a 43.17% decrease in total resistance. However, the particle separation efficiency in the cyclone decreases slightly, and the cut-off particle size increases to between 1.5 and 1.72 μm.

In [105], the characteristics of three commonly used guide vanes are presented: straight spiral vanes, curved vanes, and inclined plate vanes. It was found that installing guide vanes alters the cyclone's performance by reducing pressure drop while simultaneously increasing separation efficiency. Examples of experimental and numerical studies of a cyclone separator with a tangential inlet and a spiral guide vane are presented in [106]. The results show that the spiral guide vane has a significant effect on the velocity distribution, turbulence intensity, pressure drop, and collection efficiency in the cyclone.

Various devices designed to reduce pressure losses at the inlet to the cyclone discharge pipe are presented in [107] (Figure 9). According to the authors of [107], which presents various devices for reducing pressure losses at the inlet to the discharge pipe, the use of flow straightening devices (deswillers) reduces pressure losses in the cyclone from 400–450 to 280–310 mm H_2O. In contrast, research by the authors of [108] shows that pressure losses in the cyclone can be reduced primarily through the use of flow-straightening devices manufactured by Samsung Gwangju Electronics Co. Installed inside the cyclone's outlet tube, these devices reduce the cyclone's flow losses by approximately 11%.

 doi:10.20944/preprints202606.0235.v1

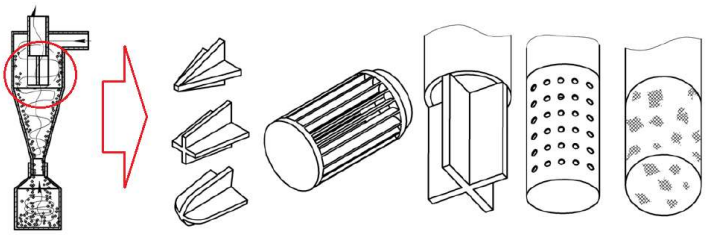

Figure 9. Components mounted at the end of the outlet pipe to reduce flow resistance in cyclones. Figure prepared by the authors using data from [107].

Article [109] presents numerical and experimental studies of two variants of a large-scale cyclone separator (CVF) with a tangential inlet and two different outlet tube diameters: 284 mm and 400 mm. Both cyclone variants were equipped with an innovative vortex detector (SVF) featuring special vertical slits in the side wall of the outlet tube, which are intended to improve the cyclone's efficiency. The slotted vortex detector (SVF) with an outlet tube diameter of 284 mm (De284) has 38 slits, while the vortex detector with an outlet tube diameter of 400 mm (De400) has 72 slits. The slit angle is 60°, and its width is 3.5 mm.

The flow resistance of the cyclone equipped with an SVF-type vortex detector was 14.1–21.2% lower compared to the CVF detector. Both detectors had the same inlet diameter as the outlet tube, De = 284 mm, but different inlet gas velocities ranging from 14.7 to 27.2 m/s. The larger inlet diameter of the SVF detector (De = 400 mm) resulted in a smaller (approximately 21.7–27.9%) pressure drops in the cyclone than in the separator with the CVF detector.

The filtration efficiency of cyclone separators with CVF and SVF vortex detectors varied significantly depending on the inlet gas velocity. Cyclone separators with SVF-type vortex detectors achieved higher and more stable filtration efficiency values.

More new modifications of the tangential inlet reverse cyclone vortex detector configuration and their impact on its performance can be found in the work of [92].

2.3. Modification of the Cyclone Design as a Result of Changes in the Configuration of the Discharge Opening and the Shape of the Dust Collector

The problem of dust accumulation in a single cyclone settling chamber and the impact of the settling chamber dimensions on the efficient operation of cyclones are presented in [110–117]. Research is conducted in two directions: configurations of dust settling chambers of various sizes and shapes [110–113] and the search for an appropriate cone geometry and installation position in the dust intake opening [114–116]. The purpose of this element, also known as the apex cone, is to limit the secondary circulation of separate dust particles. Precise selection of the cone diameter, apex angle, and its proper position are crucial. Improper selection of these parameters may block the lower outlet of the cyclone and make it difficult for dust to enter the settling tank, thus reducing the cyclone separation efficiency.

The authors of [111], after investigating the effect of the height and cylindrical diameter of the dust settling chamber on cyclone efficiency, concluded that a dipleg design with an elongated lower section connecting the cyclone to the dust settling chamber exhibits better filtration efficiency than a conventional cyclone. The authors [112] numerically investigated the effect of various cylindrical dipleg shapes on filtration efficiency characteristics and flow resistance in the cyclone. It was found that the cylindrical dipleg exhibited the highest flow resistance. At the same time, it was shown that a cyclone without a dipleg has the lowest flow resistance. It was found that the highest filtration efficiency is achieved by a cyclone with a cone-shaped dipleg, while a rhombus-shaped dipleg resulted in the lowest filtration efficiency of the cyclone.

In [114], the effect of fifteen geometric variants of a counter-rotating cone configuration on cyclone efficiency was analyzed. The cone parameters were determined using the following

 doi:10.20944/preprints202606.0235.v1

dimensions: base diameter D_S (368, 436, 520 mm), apex angle α (85, 95, 105°), and the length from the cone base to the cyclone outlet opening in its lower part with a diameter of B_h (0.1B, 0.15B, 0.35B) for a cyclone outlet opening diameter of B = 550 mm. It was found that an increase in cyclone efficiency was achieved regardless of the cone's position. Based on the results obtained, it was determined that the optimal position of the cone, considering the criterion of maximum separation efficiency, should be significantly above the lower outlet opening of the cyclone at a distance of B_h = 0.15B (82.5 mm). The angle at the apex of the cone, however, should be α = 85°. It was found that the increase in separation efficiency is noticeable for particles smaller than 60 μm, and particularly for particles smaller than 15 μm.

In [115,116], the effect of the geometry of a counter-rotating cone located at the dust outlet of a cyclone was investigated as the apex angle varied over the range α = 40-80°. It was determined that the optimal apex angle for achieving maximum separation efficiency is α = 70°. Two different cone designs were studied. The first cone variant had an apex angle of α = 90°. The cone was mounted below the lower dust outlet of the cyclone. Placing the cone (α = 120°) above the lower dust outlet of the cyclone resulted in an increase in separation efficiency of 2%. However, this caused an increase (approximately 200 Pa) in flow resistance to about 1400 Pa.

2.4. Modification of the Cyclone Design by Using Additional Elements Inside the Cyclone Separators or by Using Original (Unconventional) Cyclone Design Solutions

The efficiency of a tangential-inlet reverse cyclone can also be improved of the reverse cyclone with tangential inlet can also be achieved by using original (unconventional) cyclone design solutions [117–121]. In [117], a design of a gas-liquid cyclone is presented, characterized by generating a swirl flow using guide vanes attached to the central core and a unidirectional flow. The authors of the study note that increasing the lion's distance l_w aids in the separation of large aerosol droplets, whereas systematically reducing the outlet angle α or increasing the deflection angle β of the vanes leads to an increase in tangential velocity. This may result in improved separation efficiency in the cyclone. However, this measure causes a sharp increase in flow resistance within the cyclone. When the diameter of the cyclone's cylindrical section D_c is increased, the increase in tangential and axial velocities is correspondingly greater, which also leads to a significant increase in pressure drop.

In [118], an unconventional solution for a reverse cyclone with a tangential inlet, called PoC, was presented. The PoC configuration consists of two annular elements placed vertically at the outlet of a conventional cyclone. The outlet pipe with a diameter d_w = 100 mm downstream of the cyclone was provided with a container. A short section of cylindrical pipe 3 with a diameter d_{wp1} = 120 mm was tightly connected to the outlet pipe, leaving a gap in the upper part of the container.

A stream of air flowing out of the cyclone with a swirling motion still contains contaminants, some of which are separated and pass through the created gap 5 into the hopper space, from where they are removed by ejection. The authors of [118] investigated the application of such a solution (referred to in the literature as "Post Cyclone" PoC) in a single cyclone with a diameter D = 200 mm and height H = 850 mm for three different diameters d_{wp1} (120; 135; 150 mm) and d_{wp2} (210; 266; 310 mm) and with an ejection suction degree in the range m_{0P} = 10-25%. They used hydrated lime $Ca(OH)_2$ particles with a density of 2.45 g/cm^3 as test dust. For m_{0P} = 20% and a cyclone inlet velocity of υ_0 = 4.9-23.2 m/s, they observed changes in cyclone efficiency in the range of φ_c = 63-83%, and with a hopper at the outlet, φ_{cp} = 70-88%, with higher efficiency values obtained for smaller d_{wp1} diameters, higher m_{0P} extraction ratios, and higher υ_0 velocities.

Dust separation in the PoC occurs primarily through particle centrifugation in a tangential velocity field. Experiments have shown that, depending on operating conditions and cyclone size, PoC increases overall cyclone efficiency by 20%. The flow resistance in the PoC element is approximately 10% of the total flow resistance in the cyclone and is independent of the flow rate within the tested range. Reference [119] reports the results of a performance evaluation of a cyclone whose exhaust pipe is filled with granules, which significantly increases the filtration efficiency of all

 doi:10.20944/preprints202606.0235.v1

particle sizes at a flow rate of 10 l/min. However, at flow rates of 30 and 50 l/min, the granules only increase the collection efficiency of small particles and slightly reduce the collection efficiency of large particles.

The authors presented tests of reverse cyclone with tangential air flow to supply a square cross-section for different Reynolds numbers and three different dust grain densities (1100, 2100, and 2800 kg/m^3) and for different prismatic section heights. The final results indicate that the 4.0D model, where D is the cross-sectional dimension, outperforms all variants and showed the best performance, especially for low-density particles.

To improve the filtration efficiency of a cyclone separator, study [122] presents research on a cyclone design featuring an outlet tube positioned eccentrically relative to the cyclone's main axis. The inlet opening of the outlet tube was terminated with a symmetrical cone, and in the second case with an asymmetrical cone. This second version was called the double eccentric design. This design is characterized by the fact that the outlet tube is located in the lower right corner (top view) of the cyclone's cylindrical section. It was determined that the optimal solution is an outlet tube with an inlet diameter D_{ei} = 1.92 m and a cyclone cone height h_{ec} = 0.6 m, eccentrically offset relative to the cyclone's main axis in the "x" direction L_x = 0.21 m and in the direction of the "y" axis L_y = 0.0 m, with an eccentricity angle of θ = 270°. Compared to a single-eccentric design, the double-eccentric design significantly increases filtration efficiency but slightly increases the pressure drop.

2.5. Summary

The above comprehensive literature review has demonstrated that there is significant potential for improving cyclone performance in terms of enhancing separation efficiency or reducing flow resistance. These improvements can be achieved by modifying the design of selected cyclone components while maintaining their overall dimensions.

The proposals for structural changes to the inlet duct and outlet pipe of the cyclone presented in the literature have been evaluated mainly through numerical studies, with experimental validation being rarely validated experimentally because of high testing costs.

Studies of various shapes and sizes of dust collectors (diplegs) have shown that the geometry of the dipleg significantly affects the pressure drop in the cyclone and the filtration efficiency. The presented studies do not include simulations of the ongoing removal of dust from the sedimentation tank through the use of the ejection phenomenon.

Tangential-inlet reverse cyclones, which are components of an inertial dust collector (multicyclone) serving as the initial stage of filtration for the intake air of engines in special-purpose vehicles and work machines, can be structurally modified to increase their filtration efficiency by applying the following methods and solutions:

- modification of the shape and geometry (cross-section) of the air supply duct,
- modification of the shape of the cyclone outlet tube,
- modification of the inlet opening of the outlet tube.

The modifications presented in the literature were mainly aimed at industrial applications. To a small extent, cyclone modifications are used in motor vehicle air filters. For this reason, the authors of this paper presented in Section 3 a design for modifying the structure of a reverse cyclone with a tangential inlet, which is a component of a special vehicle multicyclone. They conducted an experimental evaluation of two modifications on a test bench in terms of efficiency and pressure drop using ejector dust extraction from the cyclone sedimentation tank, which showed an improvement in cyclone efficiency and a reduction in flow resistance. Thus, this demonstrated that it is possible to modify small cyclones (D=40 mm) to improve their performance. Despite the high cost and labor intensity of the research, experimentation remains the most reliable research method.

 doi:10.20944/preprints202606.0235.v1

3. Own Experimental Research on Cyclones

The aim of the study was to experimentally evaluate the effect of modifications to the design of a tangential-inlet reverse cyclone on its filtration efficiency and pressure drop as a function of airflow (inlet velocity υ_0) for a constant dust extraction rate from a dust collector.

3.1. Materials and Methods

The study investigated a tangentially inlet reverse cyclone, a component of a multi-cyclone intake air filter for a crawler transporter engine used in conditions of high air dustiness. The cyclone is constructed of four light alloy components: a truncated cone-shaped body, to which an inlet port is tangentially connected in the upper (wider) section, through which contaminated air is drawn in (Figure 10). The port has symmetrically rounded inlet edges, and its axis is inclined at an angle of $\gamma \cong$ 65° relative to the main cyclone axis. The cross-section of the nozzle is an ellipse A_0 with axes a = 12 and b = 15 mm. The third element of the cyclone is the outlet tube, located centrally in the cyclone's main axis and tightly secured in the cyclone's top cover. The outlet tube inlet opening is located at a distance h from the cyclone's top cover.

The 39 cyclones of the presented design form a multi-cyclone, arranged horizontally in three rows of 13 cyclones each. The cyclone outlet tubes are tightly connected by a common tank, from which the clean air is drawn in by the engine. The lower cylindrical sections of the cyclone housing are tightly secured in a common plate, which serves as the dust collector wall, from where the separated dust is removed by the suction stream generated by the exhaust gas flow. The multi-cyclone is tightly enclosed on all sides, and the ambient air enters through a rectangular opening. The cyclone inlets are positioned to allow air to be drawn from the largest (free) volume.

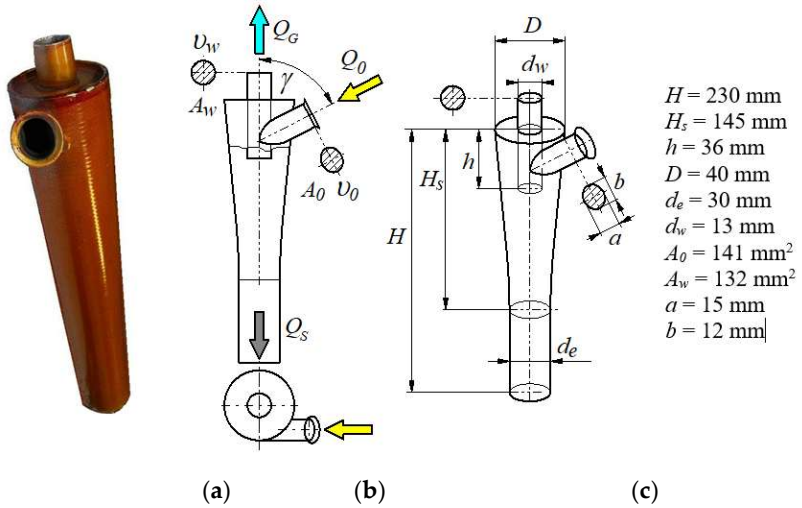

Figure 10. A counter-rotating cyclone with tangential air inlet of the crawler transporter engine: (**a**) view, (**b**) functional diagram of a cyclone, (**c**) main dimensions of the cyclone.

Design of a return cyclone for a tracked conveyor is simple. This allows for extensive modifications to the cyclone's design, which can lead to increased filtration efficiency or reduced pressure drop. It was assumed that design changes should not affect the cyclone's basic dimensions, as this could have the opposite effect. Furthermore, modified cyclones should not affect the basic design of the multi-cyclone and filter. The following modifications to the original M0 version of the reverse cyclone with a tangential inlet for a tracked vehicle were proposed (Figure 11):

 doi:10.20944/preprints202606.0235.v1

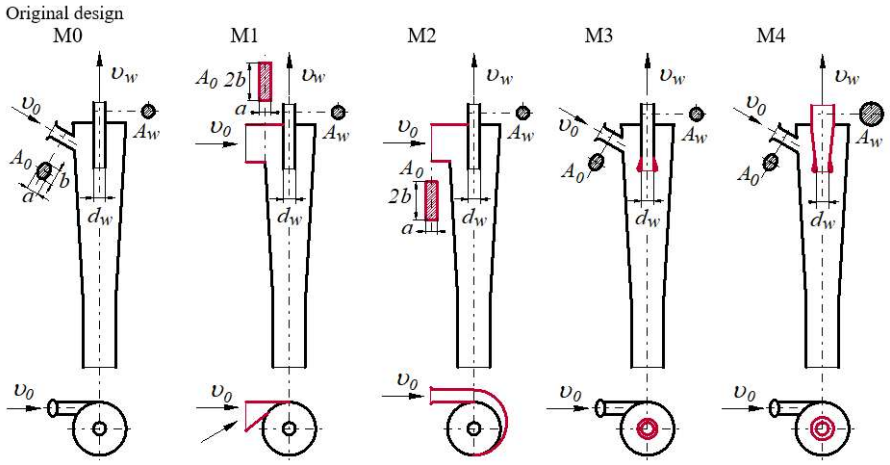

Figure 11. Possible modifications to the air filter cyclone of a tracked transporter engine.

M1 – Replacement of the diagonal cylindrical inlet duct with a tangential curved duct having a rectangular cross-section.

M2 – Replacement of the diagonal cylindrical inlet duct with a tangential inlet having a rectangular cross-section that wraps around the main body of the cyclone.

M3 – Rounding the edges of the inlet opening of the cylindrical outlet pipe of the cyclonic separator.

M4 – Replacing the cylindrical outlet pipe of the cyclonic separator with a conical pipe and rounding the edges of the inlet opening.

Figure 12b shows modification M1, which involves changing the shape of the inlet nozzle from a symmetrical diagonal to an asymmetrical curved shape with a rectangular cross-section perpendicular to the main cyclone axis of the cyclone. The cross-section of the nozzle is rectangular with dimensions 2b and a_x, where b is the longer diameter of the ellipse of the inlet nozzle cross-section. A narrow (vertical) inlet has been proposed, which, according to [75], results in a more favorable distribution of particles than the horizontal distribution of particles on the inlet surface of the cyclone.

The dimension a_x was selected so that the value of the cross-sectional area of the inlet A_0 remained unchanged after the modification. The purpose of this modification was to shape the inlet in such a way as to direct the incoming aerosol stream towards the outer wall of the cyclone inlet pipe, which would naturally allow a significant amount of dust to accumulate on the inner wall of the cyclone body. This may result in an increase in the filtration efficiency of the cyclone, as proven by the test results presented in [75–77].

 doi:10.20944/preprints202606.0235.v1

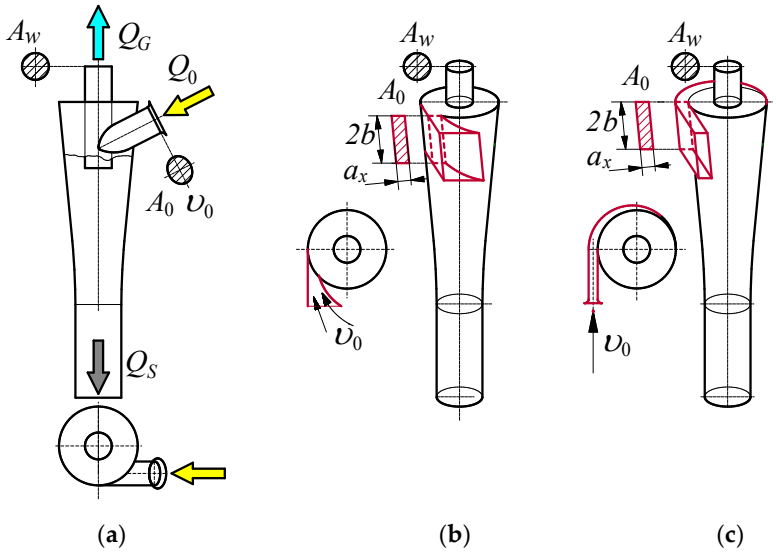

(**a**) (**b**) (**c**)

Figure 12. Air filter cyclone for crawler transporter: (**a**) original version M0 – symmetrical inlet connection shape, (**b**) curved asymmetrical inlet, modification M1, (**c**) pipe spirally wrapped around the cyclone body – modification M2.

Modification M2 involves changing the shape of the inlet nozzle from a tangential oblique inlet to a spiral inlet wrapped around the cyclone body, where the spiral wrap angle has a value of β = 180° (Figure 12c). This shape of the inlet nozzle causes the dust particles to be gently fed into the already rotating aerosol stream, which largely eliminates the interaction between the incoming and rotating aerosol streams in the cyclone. As a result of this modification, an increase in the efficiency of dust particle separation can be expected.

The M3 modification consists in replacing the cylindrical outlet pipe with the same pipe, but after eliminating the sharp edges of the inlet opening by introducing a streamlined shape in the form of a ring on the outer surface of the pipe (Figure 13).

The removal of sharp edges from the inlet opening of the outlet tube by introducing a streamlined shape eliminates the narrowing of the air flow that occurs when the flow enters an opening with sharp edges. The vena contracta effect causes a narrowing of the flow and is a direct cause of the reduction of the cross-sectional area A_k in the place through which the air flows (Figure 14). The cross-sectional area A_k is smaller than the inlet opening area A_w. This causes a local increase in flow velocity, which in turn results in an increase in the cyclone's flow resistance.

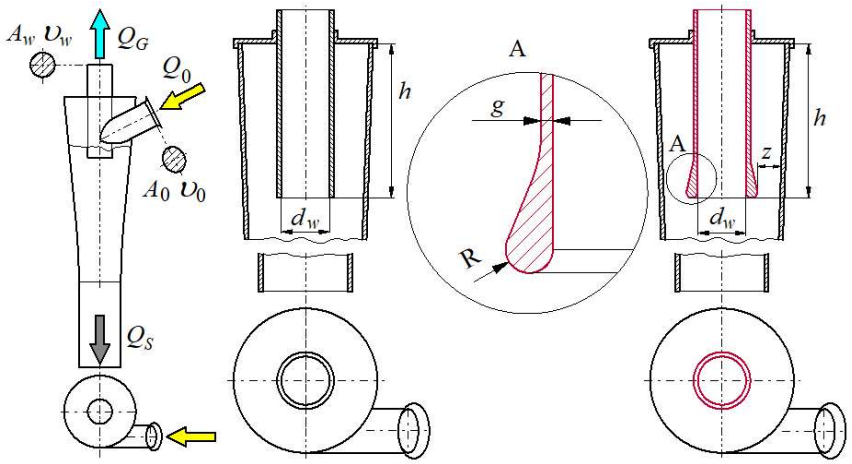

(**a**) (**b**)

 doi:10.20944/preprints202606.0235.v1

Figure 13. Air filter cyclone for a crawler transporter: (**a**) cyclone with a cylindrical outlet pipe – original version M0, (**b**) cyclone with a cylindrical outlet pipe with a streamlined inlet opening – modification M3.

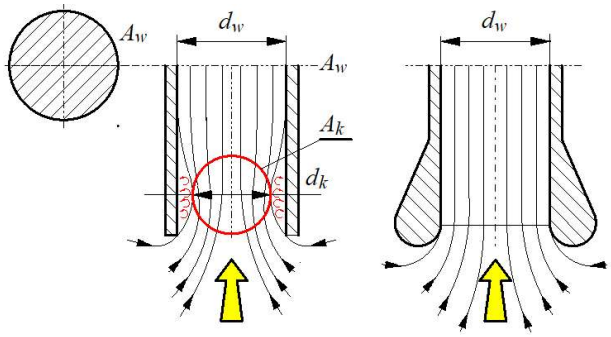

Figure 14. The phenomenon of airflow into a cylindrical duct: (**a**) an inlet opening with sharp edges, (**b**) the same duct with an aerodynamically shaped inlet opening.

The M4 modification of the cyclone was achieved by replacing the original (cylindrical) outlet tube with a truncated cone-shaped tube, while maintaining the aerodynamic shape of its inlet opening (d_w), as was done in the M3 modification (Figure 15). The cyclone outlet pipe, which has a truncated cone shape, has a smaller diameter of d_w = 13 mm, which is equal to the inner diameter of the cylindrical outlet pipe in its original shape. The diameter of the cone's outlet opening is larger, d_{w1} = 18 mm. The cone-shaped exhaust pipe was designed as a diffuser with an opening angle α_s = 7°, which is the optimal angle. At this angle, the airflow occurs without the formation of vortices and without flow separation from the duct walls. For this angle, the pressure drop coefficient is at its lowest value.

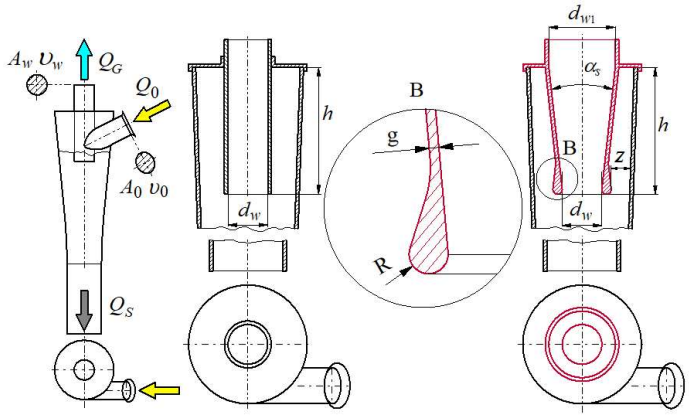

Figure 15. Air filter cyclone for a crawler transporter: (**a**) cyclone with a cylindrical outlet pipe – original version M0, (**b**) cyclone with a conical outlet pipe and a streamlined inlet opening – modification M4.

As a result of the analysis of the technological feasibility of the proposed modifications, it was concluded that modifications M1 and M2 are too technologically complex and costly to implement due to the conical shape of the upper part of the cyclone. However, proposals M3 and M4 for modifications to the design of the crawler conveyor cyclone were implemented in practice and subjected to experimental analysis.

3.1. Experimental Cyclone Research

 doi:10.20944/preprints202606.0235.v1

The study aimed to assess the impact of selected modifications to the reverse cyclone with tangential inlet on its filtration properties by experimentally determining the separation efficiency and flow resistance characteristics of the original M0 cyclone and the modified M3 and M4 cyclones. The scope of the research included determining the basic filtration characteristics:

- filtration efficiency $\varphi_c = f(Q_G)$,
- pressure drop $\Delta p_c = f(Q_G)$.

Experimental tests of cyclones were carried out on a special test bench (Figure 16), which allows the determination of filtration efficiency characteristics $\varphi_c = f(Q_G)$ pressure drop $\Delta p_c = f(Q_G)$ in the air flow range up to 85 m³/h, with a degree of ejector dust extraction from the sedimentation tank to m_0 = 20% and an airborne dust levels reaching to s = 3 g/m³ in the air sucked into the cyclone. The subject of the tests were reverse cyclones with a tangential inlet (in the original M0 version and modified M3 and M4 versions). During the tests, the cyclones were placed in a horizontal position, reflecting their original position in the air filter.

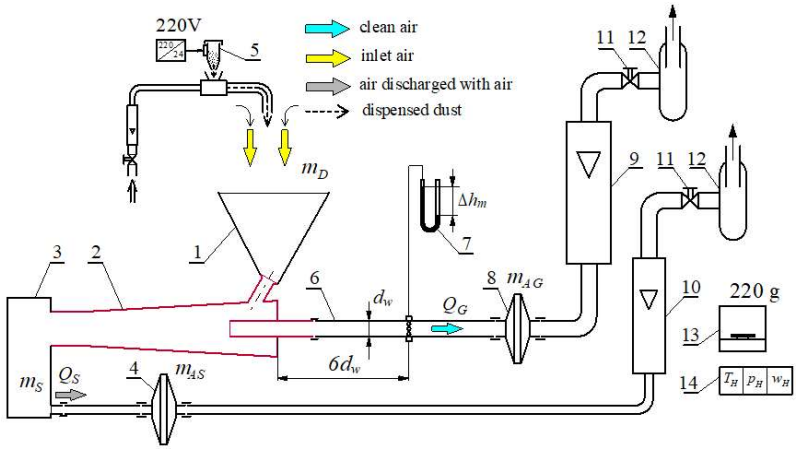

Figure 16. Cyclone test stand: 1 – dust chamber, 2 – cyclone, 3 – dust settling chamber, 4 – absolute filter, 5 – dust dispenser, 6 – cyclone pressure drop measuring duct, 7 – U-tube water manometer, 8 – absolute filter, 9, 10 – rotameters for measuring the main and suction flow, 11 – valves for regulating the air flow rate, 12 – suction fans, 13 – analytical balance, 14 – a device for measuring ambient air parameters.

A U-tube manometer is mounted on the measuring line at an appropriate distance from the clean air outlet of the cyclone, which allows the pressure drop Δhm downstream of the cyclone to be determined. The measuring line is terminated with an absolute filter, which protects the rotameter, including the float, from dust. The primary function of the absolute filter is to measure the mass of dust m_{AG} escaping from the cyclone, and thus to determine the filtration efficiency φc of the cyclone. A second absolute filter is installed in the duct extracting dust from the cyclone's dust collector. To measure the desired values of the Q_G and Q_S flows, measuring rotameters with a measuring range of Q_G = 4-64 m³/h and Q_S = 0.2-6.2 m³/h, respectively, were used.

The cyclone tests were carried out in the range of air flow Q_{Gmin}-Q_{Gmax} resulting from the number of cyclones used in the multi-cyclone air filter of the crawler conveyor and the air demand Q_F = 250-1200 m³/h by the engine of this vehicle in the speed range n_{min}-n_N. The air filter multicyclone consists of 39 elements, which provides an airflow through a single cyclone with a flow rate of Q_G = 6-30 m³/h.

The filtration efficiency of the cyclone under test was determined using the mass method during measurement cycles by weighing the mass of dust captured in the cyclone and fed into it over a fixed period of time. During the measurement, a constant air flow rate Q_G was maintained, determined using a flow meter. The measurement cycles were performed starting from Q_G = 6 m³/h in equal increments of 2 m³/h up to Q_G = 30 m³/h.

 doi:10.20944/preprints202606.0235.v1

Dust extraction from the cyclone sedimentation tank was performed using a Q_S stream. During the tests, the degree of ejection dust extraction was set at m_0 = 10%. This value was defined as the quotient of the air flow Q_S flowing in the extraction duct and the air flow Q_G flowing in the main cyclone duct [123,124].

$$m_0 = \frac{Q_S}{Q_G} 100\%. \quad (2)$$

During the tests, the principle was applied that the duration of a single measurement cycle-which corresponds to the time during which test dust is fed into the test system-is t_{pom} = 3 min. The dust was fed in such a way as to ensure a dust concentration in the inlet air of s = 1 g/m³. PTC-D test dust was used during the tests; this is a domestic substitute for AC-fine dust in terms of chemical and fractional composition.

The tests were performed for a constant air flow rate Q_G from the assumed measurement range Q_G = 6-30 m³/h of air flow. The first measurement point was the value Q_G = 6 m³/h, and subsequent measurements were performed every 2 m³/h. For each measurement point, five test cycles j = 5 were performed. After each measurement cycle, the filtration efficiency φ_{cj} of the cyclone was calculated from the following formula:

$$\varphi_{cj} = \frac{m_{Zcj}}{m_{Dcj}} 100\%, \quad (3)$$

where: m_{Zc} – mass of test dust retained by the cyclone in the assumed time, m_{Dc} – mass of dust as fed evenly into the cyclone during the measurement.

After each measurement cycle, the mass of dust m_{Dc} supplied with air to the cyclone was determined by weighing. This was the difference in mass before measurement m'_{Dc} and after measurement m''_{Dc} of the dust dispensing device container. The mass of dust retained by the cyclone m_{Zc} was determined by an indirect method after each test cycle as the mass difference:

$$m_{Zcj} = m_{Dcj} - m_{AGj} \quad (4)$$

where: m_{AGj} – dust mass retained by the filter material of the absolute filter placed in the main measuring tube. This is the difference in the masses of the absolute filter after m''_{AG} and before the measurement m'_{AG} determined by weighing with an accuracy of 0.0001 g.

The flow resistance in the cyclone Δp_c was determined as the static pressure drop in the main outlet pipe from the cyclone at a suitable distance from the cyclone body by taking readings Δh_m [mm H_2O] from the liquid manometer.

The mass content of dust in the air sucked into the cyclone during the test was calculated after the measurement was completed using the mass of the supplied dust and the formula:

$$s_j = \frac{m_{Dcj}}{Q_{0cj} \cdot t_{pom}} = \frac{m_{Dcj}}{(Q_{Gcj} + Q_{Scj}) \cdot t_{pom}} \text{ [g/m}^3\text{]}, \quad (5)$$

where: t_{pom} – time of uniform dosing of the dust mass m_{Dj} into the cyclone together with the inlet air stream.

From the five measurements performed j = 5 in the test cycle for the fixed air flow Q_G, the average values of separation efficiency φ_c and flow resistance Δp_c were calculated and then presented as characteristics in Figures 17 and 18.

 doi:10.20944/preprints202606.0235.v1

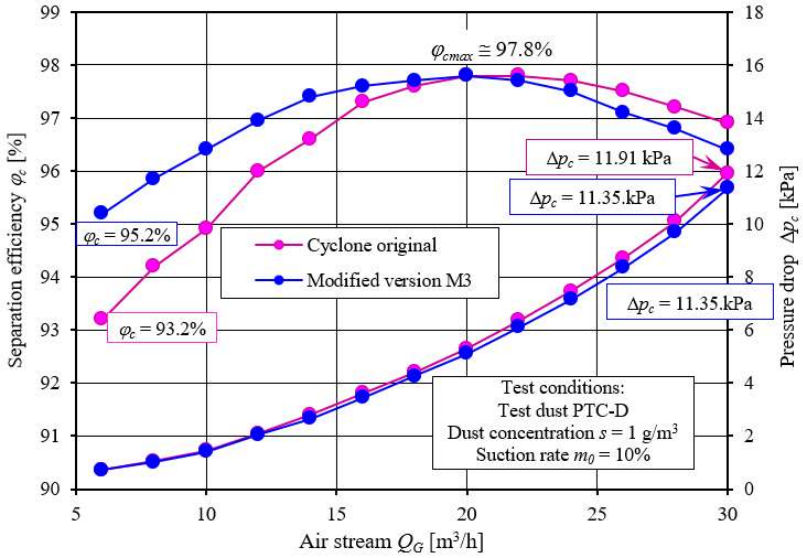

Figure 17. Characteristics $\varphi_c = f(Q_G)$ and $\Delta p_c = f(Q_G)$ original M0 and modified version M3.

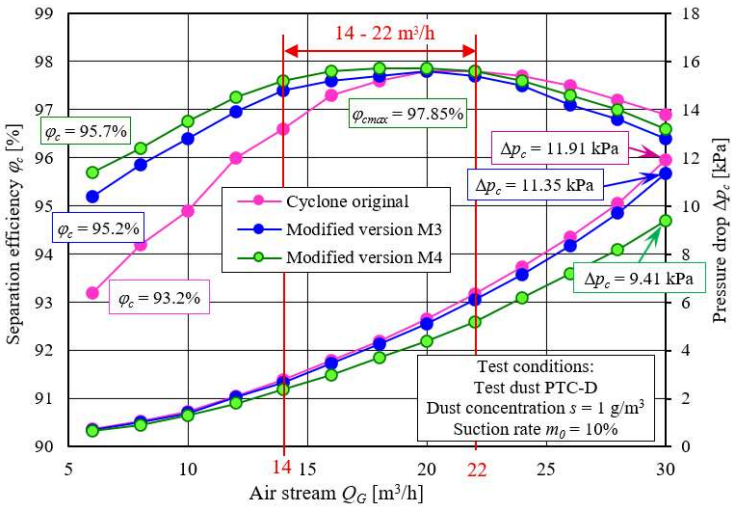

Figure 18. Characteristics $\varphi_c = f(Q_G)$ and $\Delta p_c = f(Q_G)$ original M0 and modified version M3 and M4.

3.3. Analysis of Cyclone Test Results

The characteristics of filtration efficiency $\varphi_c = f(Q_G)$ and flow resistance $\Delta p_c = f(Q_G)$ of the cyclone with the original design (M0) and the cyclone with the M3 modification are shown in Figure 17. The filtration efficiency characteristics $\varphi_c = f(Q_G)$ of the tested cyclone with the original M0 design are similar and consistent with the information provided by the authors' previous studies [49,95]. With an increase in air flow and, consequently, an increase in the inlet velocity of the cyclone, an increase in filtration efficiency up to a certain maximum value is observed. However, in the final phase of the cyclone's operation, a slight decrease in efficiency can be observed. Maximum filtration efficiency is reached at $\varphi_{cmax} \cong 97.8\%$ for an air flow rate of Q_G = 20-22 m³/h. The course of the characteristic $\varphi_c = f(Q_G)$ is typical for reverse cyclones with a tangential air flow into the cylindrical part of the cyclone and results mainly from the interdependence between the inertia force F_B and the drag force of the medium F_R. A systematic increase in the air flow through the cyclone (increase in flow velocity) results in an increase in the values of both main forces. In the flow range Q_G = 6-22 m³/h, the increase in the F_B force occurs more rapidly, resulting in a continuous increase in the cyclone's filtration efficiency.

 doi:10.20944/preprints202606.0235.v1

At higher air flow rates, a decrease in filtration efficiency is observed in many cyclones. In the cyclone tested, this phenomenon occurred after exceeding a flow rate of Q_G = 20 m³/h. The reason for this may be the faster increase in aerodynamic force P_R than inertial force P_B. This phenomenon affects dust particles with low density but high volume. As a result, the movement of the particles towards the inner wall of the cyclone is slowed down, which in turn may cause them to be carried by the rotating air stream towards the cyclone outlet pipe. Another reason for the decrease in filtration efficiency at high flow rates (for the cyclone under test, this is υ_{0max} = 65 m/s) may be the phenomenon of dust particles rebounding from the inner wall of the cyclone, towards which the particles are directed at high speed. The rebounded particles may be carried away by the internal air vortex directed towards the cyclone outlet.

The increase in air flow results in a parabolic increase in flow resistance, which results from the square of the increase in inlet velocity υ_0. For an air flow rate of Q_G = 30 m³/h, the flow resistance of the original cyclone is Δp_c = 11.9 kPa. The obtained flow resistance value is several times higher than that of other cyclones used for filtering the intake air of motor vehicle engines. At the same air flow rate, the flow resistance of other reverse cyclones with tangential or axial inlet does not exceed 2.5 kPa, and the resistance of straight-through cyclones is approximately 0.4-0.6 kPa [46,98]. At the same time, the filtration efficiency of these cyclones is significantly lower than that of the cyclone under test. Aerosol filtration in cyclones, as well as in partition filters, is characterized by the fact that the parameters of the filtration process: efficiency and flow resistance are interdependent. An increase in filtration efficiency entails an increase in flow resistance and vice versa.

The filtration efficiency characteristic $\varphi_c = f(Q_G)$ of the cyclone, where the M3 outlet pipe was modified, follows a similar curve to that of the original cyclone, but with different values (Figure 17). The introduction of a streamlined inlet opening in the cylindrical outlet pipe (M3) resulted in an approximately 2% increase in cyclone efficiency φ_c in the lower range (Q_G = 6-22 m³/h) and a slight decrease in efficiency after exceeding an air flow rate of Q_G = 20 m³/h.

For Q_G = 6 m³/h, the cyclone filtration efficiency after introducing modification M3 is φ_c = 95.2% (before modification φ_c = 93.2%), which gives an increase in efficiency of over 2%. However, for Q_G = 30 m³/h, the filtration efficiency after the introduction of modification M3 is φ_c = 96.4%, which is only 0.052% less than before the modification. The increase in filtration efficiency in the low flow range is the result of the narrowing "z" that was created after the streamlined ring was made on the outer surface of the outlet pipe. The presence of the ring on the outlet pipe reduced the free cross-section between the pipe and the cyclone cut-off. Thus, dust particles moving near the outer surface of the outlet pipe in a spiral motion down the cyclone encounter the surface of the ring, from which they are deflected from, experiencing additional acceleration towards the cyclone wall, where they are retained. In the absence of the ring (original version), these particles would be carried away by the internal vortex heading towards the outlet pipe. It can be assumed that dust particles with a low mass are subject to reflection from the ring, which in the original cyclone were carried away by the vortex, and therefore the efficiency of the cyclone in the original version is lower.

The modification of the M3 cyclone does not change the characteristics of $\Delta p_c = f(Q_G)$, in terms of its course, but changes its values, which are slightly lower across the entire air flow range. For a flow rate of Q_G = 30 m³/h, the flow resistance of the cyclone with the M3 modification is Δp_c = 11.35 kPa, which is 0.55 kPa (4.6%) lower. The reduction in flow resistance is the result of eliminating the contraction phenomenon by using a streamlined inlet opening of the outlet tube instead of an opening with edges.

Figure 18 shows the test results for modifications M3 and M4 of reverse cyclone with artificial air supply to the cylindrical part in relation to the characteristics of the cyclone in its original version.

The filtration efficiency characteristics $\varphi_c = f(Q_G)$ of the cyclone, where modification M4 of the outlet pipe was made, follow a similar pattern but with different values. Replacing the cylindrical outlet pipe with a conical one with a streamlined inlet opening (M4) resulted in a noticeable increase in the filtration efficiency φ_c of the cyclone in the lower range (Q_G = 6-22 m³/h) and a slight decrease in efficiency after exceeding an air flow rate of approximately 20 m³/h.

 doi:10.20944/preprints202606.0235.v1

Thus, the maximum efficiency of the cyclone shifted slightly towards lower Q_G values, and the characteristic $\varphi_c = f(Q_G)$ became more "flat." This indicates that it makes sense to use such design solutions in cyclones.

The application of the M4 modification to the cyclone outlet pipe resulted, as expected, in a significant reduction in flow resistance $\Delta p_c = f(Q_G)$ of the cyclone across the entire range of the tested air flow Q_G, compared to the original version (approximately 20%). For a flow rate of Q_G = 30 m³/h, the flow resistance of the cyclone with the M4 modification is Δp_c = 9.41 kPa, which is 0.55 kPa (21%) lower. The decrease in flow resistance was caused by the introduction of modification M4 results from a 50% reduction in the outlet velocity υw of the cyclone (from υ_w = 65.0 m/s to υ_w = 32 m/s for Q_G = 30 m³/h) as a result of replacing the cylindrical outlet pipe d_w = 13 mm with a conical one with an outlet diameter d_{w1} = 18 mm. The reduction in flow resistance was also caused by the introduction of a streamlined shape of the inlet opening of the outlet pipe.

The results of the tests presented in Figure 18 show that the tested cyclone should operate within a narrow range of air flow changes Q_G = 14-22 m³/h, which results from the maximum efficiency of dust particle filtration and relatively low flow resistance in this range. Extending the cyclone's operation above Q_G = 22 m³/h results in decreasing efficiency and a sharp increase in flow resistance. Excessive flow resistance of cyclones causes an increase in flow resistance in the engine intake system, which can result in a decrease in engine filling and power. Cyclone operation at lower filtration efficiency will increase the mass of dust fed to the second stage of filtration (pleated paper filter), thus causing an accelerated increase in flow resistance and shortening its operating time until the permissible resistance is reached.

3.4. Analysis of Cyclone Filtration Efficiency Calculation Results

During the tests, varying changes in filtration efficiency and flow resistance were found in the tested cyclone models: in the original version and with the M3 and M4 design modifications. The data presented in Figures 17 and 18 show that there is a close relationship between the filtration efficiency and flow resistance of cyclones. An increase in cyclone filtration efficiency is usually associated with an increase in flow resistance. It is difficult to directly compare the filtration properties of cyclones in this respect. Therefore, the filtration quality factor q_c, which refers to the filtration efficiency and flow resistance of the same filter material or filter element (cyclone), is commonly used in the literature. According to [126,127] the filtration quality factor is expressed by the following relationship:

$$q_c = \frac{-\ln(1-\varphi_c)}{\Delta p_c} [1/\text{kPa}] \qquad (6)$$

where: φ_c – cyclone filtration efficiency, Δp_c – cyclone flow resistances [kPa].

A higher q_c coefficient value indicates a more favorable relationship between filtration efficiency and flow resistance, which means a more effective filtration process.

Figure 19 shows the values of the filtration quality coefficient q_c for the basic M0 cyclone and cyclones with structural modifications M3 and M4. As the air flow Q_G passing through the cyclone increases, the filtration quality coefficient q_c of the tested cyclone versions decreases. Regardless of the cyclone variant tested, the highest filtration quality coefficient q_c values are achieved by the cyclone with the M4 design modification, which resulted in a noticeable increase in efficiency, especially in the range of low Q_G flow rates, and a significant decrease in flow resistance. According to equation (6), the filtration quality coefficient qc determined for Q_G = 6 m³/h takes the following values for cyclone variants M0, M3, and M4, respectively: q_{cM0} = 3.73 kPa-1, q_{cM3} = 4.23 kPa-1, q_{cM4} = 4.76 kPa-1. For an air flow of Q_G = 30 m³/h, the filtration quality coefficient q_c values are an order of magnitude smaller.

 doi:10.20944/preprints202606.0235.v1

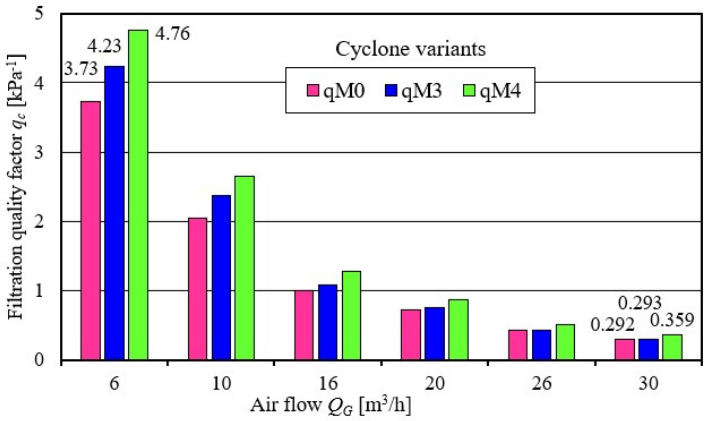

Figure 19. Filtration quality coefficient q_c of the basic M0 cyclone and cyclones with structural modifications M3 and M4 depending on the air flow Q.

A dust particle in a cyclone is subject to two main forces resulting from its inertia F_B and aerodynamic drag F_R. The shape of the dust grain's trajectory depends on the interrelationship between these forces. The magnitude of the F_B and F_R forces depends on the particle's size and shape, the material it is composed of, and the type of medium in which it is moving. The rotational motion of the aerosol, which is the source of the particle's motion, creates a centrifugal force. The value of this force for a dust particle with mass m_p located at a distance "r" from the axis of rotation is given by the relationship [128,129]:

$$F_B = \frac{m_p \cdot u_s^2}{r}, \quad (7)$$

where: u_s – the tangential velocity of the grain, which approximately corresponds to the value of the tangential velocity of the gas υ_S.

The inertial force directs the dust grain towards the inner wall of the cyclone at the velocity u_r. The drag force of the medium F_R, which is opposite to this movement, is determined by the relationship [129]:

$$F_R = \frac{18\mu_g}{\rho_p d_p^2} \cdot \frac{\rho_g Re}{24}, \quad (8)$$

where: ρ_p – dust grain density, ρ_g – the density of the medium in which the particle moves, d_p – dust particle diameter, μ_g – gas viscosity.

According to Newton's law applied to the radial motion component u_r, with resistances directed towards the interior (axis) of the cyclone, the equation of motion of the particle will take the form [129]:

$$m_p \cdot \frac{du_r}{dt} = \frac{m_p \cdot u_s^2}{r} - F_R. \quad (9)$$

Dust particles of varying sizes are directed into the cyclone along with the airflow due to the polydispersity of the dust and varying densities resulting from its chemical composition. Particles of the same size but with different densities have different masses, and therefore different inertia forces. Dust particles larger than a certain d_{pg} dimension, defined as the cutoff diameter, for which $F_B > F_R$ will move in a spiral path and, after several rotations, reach the inner wall of the cyclone. These particles are assumed to be separated with 100% efficiency. However, dust particles smaller than a certain d_{pg} dimension, for which $F_B < F_R$ applies, will be entrained by the internal vortex of the airflow towards the cyclone outlet tube. The separation efficiency of these particles in the cyclone is therefore 0%. At the same time, it is assumed that particles whose dimension is equal to d_{pg}, for which the force F_B and the force F_R are equal, will (theoretically) orbit in a circle of radius "r".

Dust particles have a very irregular shape, which significantly influences the drag force of the medium, and are characterized by varying densities, which influence their mass and, consequently, the centrifugal force. Therefore, particles for which $F_B = F_R$ do not move infinitely in a circle with a defined radius. It is assumed with great probability in the literature that 50% of them are retained in

 doi:10.20944/preprints202606.0235.v1

the cyclone, and 50% are entrained by the internal vortex flowing to the cyclone outlet. It is also assumed that the size of dust particles that demonstrate 50% efficiency is called the cut-off diameter d_{pg} and is conventionally designated as d_{50} [130,131].

The cut off diameter d_{pg} is a measure of the structural quality of a cyclone and depends mainly on the main dimensions of the cyclone and the parameters of the flowing aerosol. It is the minimum diameter of dust particles that are still removed from the flowing gas under specific cyclone operating conditions. For fixed flow conditions (constant gas flow rate Q_G), theoretically only dust particles below a certain d_{pg} limit size should be present in the air behind the cyclone.

The dpg value can be determined from a theoretical relationship. One of the most commonly used formulas for determining the cut off diameter d_{pg} is [96]:

$$d_{pg} = \sqrt{\frac{18\mu_g r \mu_r}{\rho_p \upsilon_s}}. \qquad (10)$$

This relationship was reformulated by the authors to the following form:

$$d_{pg} = \frac{3}{2}\sqrt{\frac{A_0}{A_w}\frac{D}{\upsilon_0}\left(\frac{D}{d_w}\right)^{-(2m+1)}\left(\frac{h_w}{d_w}\right)^{-1}\frac{\mu_g}{\rho_p}} \qquad (11)$$

where: A_0 – cross-sectional area of the inlet duct, A_w – cross-sectional area of the outlet duct, D – cyclone diameter, d_w – inlet diameter of the outlet pipe, m – exponent of the equation ranging from 0.5 to 0.9.

For the tested cyclone, calculated from the relationship (11) for an air flow of 30 m³/h and for basic dust components that differ in density (SiO_2, Al_2O_3, Fe_2O_3), the cut off diameter d_{pg} take the values shown in Table 2.

Table 2. Results of calculations of the cut off diameter d_{pg} of dust particles for the basic version of the cyclone.

Q_G [m³/h]	υ_0 [m/s]	d_{pg} [µm]		
		SiO_2 ρ_p = 2650 [kg/m³]	Al_2O_3 ρ_p = 3990 [kg/m³]	Fe_2O_3 ρ_p = 5240 [kg/m³]
6	13.0	0.531	0.432	0.377
10	21.7	0.411	0.335	0.292
16	34.7	0.325	0.265	0.231
20	43.3	0.291	0.237	0.206
26	56.3	0.255	0.208	0.181
30	65.0	0.237	0.193	0.169

The calculated cut-off diameters d_{pg} differ slightly from each other and take on very small values (0.531-0.169 µm). As the airflow Q_G through the cyclone increases, the characteristic grain size dpg decreases. The same relationship occurs as the dust particle density increases. Both of these phenomena confirm the cyclone's proper particle separation performance.

This phenomenon should be explained by the fact that the PTC-D test dust (which is an equivalent of road dust) is not only a dust with a diverse chemical composition but is also a polydisperse dust. Therefore, the dust particles have different sizes in the range of d_p = 0-80 µm, different shapes other than spherical, and different densities. Therefore, dust particles of the same size (having the same volume) have different masses, which determines their inertial force. A particularly unfavourable P_R and P_B force ratio occurs for dust particles with low mass and high volume (low density). Thus, assuming that the shape of the particles has no effect on the medium resistance force P_R particles with higher density, such as iron oxide or corundum, will be more effectively separated in the cyclone.

 doi:10.20944/preprints202606.0235.v1

3.5. Summary of the Design Modification Tests for the Tangential Inlet Reverse Cyclone

A two-stage modification of the tangential inlet reverse cyclone design was performed. This involved replacing the cylindrical outlet tube (d_w = 13 mm) with a truncated cone-shaped tube, the smaller diameter of which equals the inner diameter of the outlet tube dw, and the larger diameter d_{w1} = 18 mm, while simultaneously streamlining the edges of the inlet opening dw. Using a specialized test rig, the effect of the introduced cyclone modifications on its filtration efficiency and flow resistance was experimentally assessed. The tests were conducted with high concentrations of test dust with grain sizes up to 80 μm and a SiO_2 content of over 67%, using continuous dust extraction from the cyclone's settling chamber.

The filtration efficiency characteristics $\varphi_c = f(Q_G)$ of the tested cyclone show an increase in filtration efficiency up to a certain maximum value. However, a slight decrease is observed in the final phase of cyclone operation. This filtration efficiency curve is consistent with information provided by the authors of other research studies. The presented test results indicate that the tested cyclone should operate within a narrow airflow range of Q_G = 14-22 m³/h. This ensures maximum dust particle filtration efficiency and relatively low flow resistance within this range. Extending the cyclone's operation above Q_G = 22 m³/h and below Q_G = 14 m³/h results in decreased filtration efficiency, while operating the cyclone above Q_G = 22 m³/h results in an increase in flow resistance from 5.25 kPa to 9.41 kPa, i.e., by over 75%.

Compared with the original version, filtration efficiency increased by 2.7% in the lower airflow range and a significant (over 20%) decrease in flow resistance $\Delta p_c = f(Q_G)$ of the cyclone across the entire Q_G airflow range tested. The research conducted indicates possible directions for modifying the design of reverse cyclones with tangential inlets.

4. Conclusions

The aim of this work was to theoretically and experimentally evaluate a practical modification of the reverse cyclone design with a tangential airflow inlet in terms of efficiency and flow resistance. The cyclone is a component of a multi-cyclone air filter for a special vehicle. A literature review demonstrated the existence (over many years) of experimentally established mathematical relationships between the main dimensions of the cyclone. These are the appropriate proportions (quotients of the main dimensions) that ensure the cyclone achieves maximum filtration efficiency and minimum resistance. Any change to these proportions in an existing cyclone can have negative consequences on its performance.

For this reason, improving cyclone efficiency by reducing flow resistance or increasing filtration efficiency can only be achieved by modifying its design. Data presented in the literature clearly indicate that the cause of the largest pressure losses during gas flow in a cyclone are energy losses occurring during flow through the cyclone outlet tube. An extensive literature review shows that the use of a streamlined inlet opening of the outlet pipe and a conical outlet pipe instead of a cylindrical one brings measurable effects in terms of the efficiency and flow resistance of a reverse cyclone with a tangential inlet.

Two modifications of the reverse cyclone outlet pipe with a tangential inlet were made and their experimental evaluation in terms of filtration efficiency and flow resistance was carried out. This allowed the following conclusions to be drawn.

1. There are many design options for increasing cyclone efficiency, but not all solutions, due to their complex design, can be used in cyclones used in motor vehicle engine intake air filters. The effect of increased filtration efficiency or reduced flow resistance may be disproportionately small compared to the costs incurred.
2. The following practical solutions can be used to modify cyclones used in the intake air filters of motor vehicle engines: eliminating sharp edges in the inlet opening of the exhaust pipe by giving

 doi:10.20944/preprints202606.0235.v1

it a streamlined shape and changing the exhaust pipe from its cylindrical shape to a conical one. The feasibility of such modifications was confirmed experimentally.

3. The filtration efficiency of reverse cyclones with the air flow supplied tangentially to the cylindrical part through a duct and the use of polydisperse dust increases with the increase in flow velocity υ (air flow Q_G) until reaching a maximum value of $\varphi_{cmax} \approx 97.85\%$ and then decreases slightly. This characteristic of the $\varphi_c = f(Q_G)$ curve and the obtained efficiency values are consistent with data presented in the literature and confirmed by the authors of many research works [47,93,121], as well as with other research results by the author [44,45,95].
4. Modifying the cyclone design does not change the fundamental characteristics φ_c and Δp_c. The effect of the modifications to the cyclone design is primarily a significant (over 20%) decrease in flow resistance across the entire range of the tested airflow Q_G and an approximately 2% increase in filtration efficiency φ_c in the lowest airflow Q_G values.
5. The conducted research confirmed that it is possible to improve cyclone efficiency without altering its main dimensions to reduce flow resistance or increase filtration efficiency. Therefore, future work will focus on the configuration of the cyclone inlet duct, which may result in a further reduction in cyclone flow resistance.

The development of tangential inlet cyclones has been ongoing since their design and operation were patented over 100 years ago. The basic design of the tangential inlet cyclone has remained unchanged to this day, although work is constantly being carried out to increase the efficiency of aerosol particle separation. The efficiency of a cyclone separator depends on many factors. These include geometric parameters represented by the design dimensions of the cyclone, gas flow parameters (cyclone inlet velocity, temperature, viscosity and density of the gas), and dust parameters (chemical and fractional composition, grain density and shape). Cyclones have a wide and varied range of applications, so their development depends on the tasks they have to perform. Cyclones are primarily required to be highly effective and have low flow resistance. It is difficult, and sometimes impossible, to meet these requirements simultaneously. Increasing filtration efficiency will focus on the use of several cyclone inlets, cyclone inlets wrapped around the cylindrical part, diagonal inlets, continuous dust extraction from the cyclone sedimentation tank, the use of an electric field, and the use of additional swirlers in the outlet pipes. These measures may result in increased cyclone flow resistance. Measures to reduce flow resistance will mainly focus on the shape of the outlet pipe and the installation of deflectors to reverse the flow in the outlet pipe. It should be noted that some solutions may be complex and costly, especially when considering a battery of several hundred cyclones arranged in parallel (multicyclone), in which case economic considerations may rule them out.

Author Contributions: Conceptualization, T.D. and S.D.; methodology, T.D.; software, S.D.; validation, T.D. and S.D.; formal analysis, T.D.; resources, T.D. and S.D.; data curation, S.D.; writing—original draft preparation, T.D.; writing—review and editing, T.D. and S.D; visualization, T.D.; supervision, T.D.; All authors have read and agreed to the published version of the manuscript.

Funding: This work was financed by Military University of Technology under research project EL_UGBWIM_10012026_01.

Data Availability Statement: The original contributions presented in this study are included in the article. Further inquiries can be directed to the corresponding author.

Conflicts of Interest: The authors declare no conflicts of interest.

 doi:10.20944/preprints202606.0235.v1

References

1. Dziubak, T.; Boruta, G. Experimental and Theoretical Research on Pressure Drop Changes in a Two-Stage Air Filter Used in Tracked Vehicle Engine. *Separations* 2021, 8, 71. https://doi.org/10.3390/separations8060071.
2. Dziubak, T. The influence of a filter on the filling of a piston combustion engine. Doctoral dissertation. Military University of Technology, Warszawa 1991. (in Polish).
3. Dziubak, T.; Trawiński, G. The experimental Research of the air filter flow drag influence on the T359E engine operation parameters. *Bull. Mil. Univ. Technol.* 2001, 4(584), pp. 135-149.
4. Dziubak, T.; Karczewski, M. Experimental Study of the Effect of Air Filter Pressure Drop on Internal Combustion Engine Performance. *Energies* 2022, 15, 3285. https:// doi.org/10.3390/en15093285.
5. Thomas, J.; West, B.; Huff, S. Effect of Air Filter Condition on Diesel Vehicle Fuel Economy; SAE Technical Paper 2013-01-0311; SAE International: Warrendale, PA, USA, 2013. https://doi.org/10.4271/2013-01-0311.
6. Honeywell AGT1500 - Archived 3/2009. https://www.scribd.com/document/325384791/AGT1500-Turbine-Technology.
7. Hjelm, R.; Wahlström, J.; Yenibayrak, I.; Sabani, D.; Runsten, P.; Lyu, Y. Airborne Wear Particles from Dry Clutches. *Atmosphere* 2022, 13(10):1700. https://doi.org/10.3390/atmos13101700.
8. Lee, J.; Kwon, O.; Hwang, Y.; Yeon, G. Laboratory Evaluation of Wear Particle Emissions and Suspended Dust in Tire–Asphalt Concrete Pavement Friction. *Appl. Sci*. 2024, 14, 6362. https://doi.org/10.3390/app14146362.
9. Glišović, J.; Pešić, R.; Lukić, J.; Miloradović, D. Airborne wear particles from automotive brake system: environmental and health issues. 1st International conference on Quality of Life. Kragujevac Faculty of Engineering, University of Kragujevac June 09th-10th, 2016, 289-295.
10. Wang, Y.; Yin, H.; Yang, Z.; Su, S.; Hao, L.; Tan, J.; Wang, X.; Niu, Z.; Ge, Y. Assessing the brake particle emissions for sustainable transport: A review. *Renew. Sustain. Energy Rev*. 2022, 167, 112737. https://doi.org/10.1016/j.rser.2022.112737.
11. Yoo, J.; Lee, Y. An Experimental Study on the Fine Particle Emissions of Brake Pads According to Different Conditions Assuming Vehicle Deceleration with Pin-on-Disc Friction Test. *Appl. Sci.* 2024, 14, 1000. https://doi.org/10.3390/app14031000.
12. Wagner, S.; Klöckner, P.; Reemtsma, T. Aging of tire and road wear particles in terrestrial and freshwater environments – A review on processes, testing, analysis and impact. *Chemosphere* 2022, 288:132467. https://doi.org/10.1016/j.chemosphere.2021.132467.
13. Li, J.; Zhang, M.; Ge, Y.; Wen, Y.; Luo, J.; Yin, D.; Wang, C.; Wang, C. Emission Characteristics of TyreWear Particles from Light-Duty Vehicles. *Atmosphere* 2023, 14, 724. https://doi.org/10.3390/atmos14040724.
14. Jandacka, D.; Brna, M.; Durcanska, D.; Kovac, M. Characterization of Road Dust, PMx and Aerosol in a Shopping–Recreational Urban Area: Physicochemical Properties, Concentration, Distribution and Sources Estimation. *Sustainability* 2023, 15, 12674. https://doi.org/10.3390/su151712674.
15. Lei, T.M.T.; Liu, Y.; Ye, W.; Cheng, W.H.; Molla, A.H.; Chen, L.-W.A.;Wu, S. Preliminary Findings of Heavy Metal Contents from Road Dust and Health Risk Assessments Towards a More Sustainable Future in Macao. *Sustainability* 2025, 17, 10433. https://doi.org/10.3390/su172310433.
16. Bojdo, N.; Filippone, A. Effect of desert particulate composition on helicopter engine degradation rate, 40th European Rotorcraft Forum, Southampton, Conference Paper. September 2014. https://www.researchgate.net/publication/265556798.
17. Smialek, J.L.; Archer, F.A.; Garlick, R.G. Turbine Airfoil Degradation in the Persian Gulf War. The Journal of The Minerals, *Metals & Materials Society (TMS).* 1994, 46(12), pp. 39-41.
18. Summers, C.E. The physical characteristics of road and field dust. SAE Technical Paper, 250010,1925, 10.4271/250010.1925.
19. Vogel, A.; Durant, A.J.; Cassiani, M.; Clarkson, R.J.; Slaby, M.; Diplas, S.; Krüger, K.; Stohl, A. Simulation of Volcanic Ash Ingestion Into a Large Aero Engine: Particle–Fan Interactions. *ASME J. Turbomach.* 2019, 141, 011010

 doi:10.20944/preprints202606.0235.v1

20. Dzierżanowski, P.; Kordziński, W.; Otyś, J.; Szczeciński, S.; Wiatrek, R. *Napędy Lotnicze. Turbinowe silniki śmigłowe i śmigłowcowe*; WKŁ: Warszawa, Poland, 1985. (In Polish)
21. Su, W.-H. Dust and atmospheric aerosol. Resources. *Conserv. Recycl.* 1996, 16, pp. 1–14. https://doi.org/10.1016/0921-3449(95)00045-3.
22. Juda-Rezler, K.; Toczko, B. *Pyły drobne w atmosferze. Kompendium wiedzy o zanieczyszczeniu powietrza pyłem zawieszonym w Polsce*; Biblioteka Monitoringu Środowiska: Warszawa, Poland, 2016. (In Polish)
23. Schaeffer, J.W.; Olson, L.M. Air Filtration Media for Transportation Applications, *Filtration & Separation*, 1998, 35(2), pp. 124-129.
24. Barris, M.A. *Total Filtration™: The Influence of Filter Selection on Engine Wear, Emissions, and Performance*; SAE Technical Paper Series 952557; SAE International: Warrendale, PA, USA, 1995. https://doi.org/10.4271/952557.
25. Barbolini, M.; Di Pauli, F.; Traina, M. Simulation der luftfiltration zur auslegung von filterelementen, *MTZ - Motortechnische Zeitschrift* 5(11), 52-57, 2014.
26. Jaroszczyk T.: Air Filtration in Heavy-Duty Motor Vehicle Applications. Proc. Dust Symposium III Vicksburg MS, 15-17 September 1987.
27. Dziubak, T. Zapylenie powietrza wokół pojazdu terenowego, *Wojskowy Przegląd Techniczny*. 3(257), pp. 154-157. 1990. (in Polish).
28. Burda, S.; Chodnikiewicz, Z. Konstrukcja i badania pyłowe filtrów powietrza silnika czołgowego, Biuletyn WAT, 3(115), pp. 12-34, 1962, (in Polish).
29. Durst M., Klein G., Moser N.: Filtration in Fahrzeugen. Mann+Hummel GMBH. Ludwigsburg, Germany 2005.
30. Szczeciński S.; Otyś J., Dzierżanowski P.; Wiatrek R. Turbinowe napędy samochodów. WKŁ, Warszawa 1974. (in Polish)
31. Bojdo, N. Rotorcraft engine air particle separation. A thesis submitted to the University of Manchester for the degree of Doctor of Philosophy in the Faculty of Engineering and Physical Sciences 2012. https://www.escholar.manchester.ac.uk/uk-ac-man-scw:183545.
32. Chatten, C. Sandblaster 2 support of see-through technologies for particulate brownout, Task 5 Final Technical Report, DTIC Document, 2007. https://apps.dtic.mil/sti/pdfs/ADA504965.pdf (Accessed February 6, 2026).
33. Szczepankowski, A.; Szymczak, J.; Przysowa, R. The Effect of a Dusty Environment Upon Performance and Operating Parameters of Aircraft Gas Turbine Engines, Conference: Specialists' Meeting - Impact of Volcanic Ash Clouds on Military Operations NATO AVT-272-RSM-047 At: Vilnius. May 2017. doi:10.14339/STO-MP-AVT-272-06-PDF. 10.14339/STO-MP-AVT-272.
34. Van der Walt, J.P.; Nurick, A. Erosion of dust-filtered helicopter turbine engines part I: basic theoretical considerations, *Journal of Aircraft*, 32(1), pp. 106-111. 1995a. https://doi.org/10.2514/3.56919.
35. Needelman, W.; Madhavan, P.; Review of Lubricant Contamination and Diesel Engine Wear, SAE Technical Paper 881827, 1988, https://doi.org/10.4271/881827.
36. Ali, M.K.A.; Xianjun, H.; Turkson, F.R.; Ezzat, M. An analytical study of tribological parameters between piston ring and cylinder liner in internal combustion engines. *Proc. Inst. Mech. Eng. Part K J. Multi-Body Dyn.* 2016, 230, 329-349. https://doi.org/10.1177/1464419315605922.
37. Jaroszczyk, T.; Pardue, B.A.; Heckel, S.P.; Kallsen, K.J. Engine air cleaner filtration performance—Theoretical and experimental background of testing. In Proceedings of the AFS Fourteenth Annual Technical Conference and Exposition, Tampa, FL, USA, 1–4 May 2001.
38. Nagy, J. Filtrowanie a żywotność silnika. *Siln. Spalinowe* 1973, 3, pp. 43-47. (In Polish).
39. Long, J.; Tang, M.; Sun, Z.; Liang, Y.; Hu, J. Dust Loading Performance of a Novel Submicro-Fiber Composite Filter Medium for Engine. *Materials* 2018, 11, 2038. https://doi.org/10.3390/ma11102038.
40. Jaroszczyk, T.; Fallon, S.L.; Liu, Z.G.; Scott P. Heckel Development of a Method to Measure Engine Air Cleaner Fractional Efficiency. International Congress and Exposition Detroit, Michigan March. pp. 1-4, 1999.

 doi:10.20944/preprints202606.0235.v1

41. Wróblewski, P**.** Contemporary problems of designing engines for military drone propulsion systems, taking into account their unforeseen mechanical failures and technical protection. *Military Logistics Systems*. 2025;63(2):203–224. doi:10.37055/slw/218687.
42. Dziubak, T. Research into a Two-Stage Filtration System of Inlet Air to the Internal Combustion Engine of a Motor Vehicle. *Energies* 2024, 17, 6295. https://doi.org/10.3390/en17246295.
43. Bastuck, T.; Böhnke, F.; Hoppe, S.; Mittler, R. Systemische Kolbenringauslegung zur Reduzierung von Partikelrohemissionen. *MTZ—Motortechnische Zeitschrift* 2020, 81, pp. 50–55. https://doi.org/10.1007/s35146-020-0283-z.
44. Gunkel, M.; Frensch, M.; Robota, A.; Gelhausen, R. Innermotorische Emissionsreduzierung Zusammenhang zwischen Partikelemissionen und Ölverbrauch. *MTZ-Motortechnische Zeitschrift* 2018, *79*, pp. 46-51. https://doi.org/10.1007/s35146-018-0044-4.
45. Babaoˇglu, N.U.; Parvaz, F.; Hosseini, S.H.; Elsayed, K.; Ahmadi, G. Influence of the inlet cross-sectional shape on the performance of a multi-inlet gas cyclone. Powder Technol. 2021, 384, pp. 82-99. https://doi.org/10.1016/j.powtec.2021.02.008.
46. Dziubak, T. Experimental Investigation of Possibilities to Improve Filtration Efficiency of Tangential Inlet Return Cyclones by Modification of Their Design. *Energies* 2022, pp. 15, 3871. https://doi.org/10.3390/en15113871.
47. Dziubak, T. Modification of returnable cyclone with a tangent inlet construction. *Bulletin of the Military University of Technology*. 2006, LV(2): pp. 279-301.(In Polish).
48. Dziubak, T. The problems of the filtration in the vehicle engines exploitated in large pollution conditions. Exploitation Problems of Machines. *Polish Academy of Sciences.* 2000, 4 (124): pp. 181-197. (In Polish).
49. Dziubak, S.; Małachowski, J.; Dziubak, T.; Tomaszewski, M. Numerical studies of an axial flow cyclone with ongoing removal of separated dust by suction from the settling tank. *Chemical Engineering Research and Design* 2024, 208, pp. 29-51. https://doi.org/10.1016/j.cherd.2024.05.044.
50. Babaoˇglu, N.U.; Hosseini, S.H.; Ahmadi, G.; Elsayed, K. The effect of axial cyclone inlet velocity and geometrical dimensions on the flow pattern, performance, and acoustic noise. *Powder Technol*. 2022a, 407, 117692. https://doi.org/10.1016/j. powtec.2022.117692.
51. Gopalakrishnan, B.; Arul Prakash, K. Numerical study on pressure drop and filtration efficiency of gas-solid flow through axial cyclone separators. *Int J Adv Eng Sci Appl Math*. 2019, 11(4), pp. 280-287. https://doi.org/10.1007/s12572-020-00259-5.
52. Dziubak, T. Research into a Two-Stage Filtration System of Inlet Air to the Internal Combustion Engine of a Motor Vehicle. *Energies* 2024, 17, 6295. https://doi.org/10.3390/ en17246295.
53. Dong J., Chena G., Zhang P., Li J. Separation Performance Enhancement of Gas-Solid Cyclone Separators by Flow Control and Coupling Physical Fields, Separation & Purification Reviews, 2026, 55:2, 109-124. https://doi.org/10.1080/15422119.2025.2464111.
54. Juda, J. Pomiary Zapylenia i Technika Odpylania; WNT: Warszawa, Poland, 1968.
55. Gimbun, J.; Chuah, T.G.; Choong, T.S.Y.; Fakhru'L-Razi, A. A CFD Study on the Prediction of Cyclone Collection Efficiency. *Int. J. Comput. Methods Eng. Sci. Mech.* 2005, *6*, pp. 161-168. https://doi.org/10.1080/15502280590923649.
56. Leith, D.; Mehta, D. Cyclone performance and design. *Atmosp. Environ.* 1973, *7*, 527-549. https://doi.org/10.1016/0004-6981(73)90006-1.
57. Dirgo, J.; Leith, D. Cyclone Collection Efficiency: Comparison of Experimental Results with Theoretical Predictions. *Aerosol Sci. Technol.* 1985, 4, pp. 401-415. http://dx.doi.org/10.1080/02786828508959066.
58. Ramachandran, G.; Leith, D.; Dirgo, J.; Feldman, H. Cyclone Optimization Based on a New Empirical Model for Pressure Drop. *Aerosol Sci. Technol.* **1991**, *15*, 135–148. https://doi.org/10.1080/02786829108959520.
59. Iozia, D.L.; Leith, D. The Logistic Function and Cyclone Fractional Efficiency. *Aerosol Sci. Technol.* 1990, *12*, pp. 598-606. https://doi.org/10.1080/02786829008959373.
60. Karagoz, I.; Avci, A. Modelling of the Pressure Drop in Tangential Inlet Cyclone Separators. *Aerosol Sci. Technol.* 2005, *39*, 857-865. https://doi.org/10.1080/02786820500295560.
61. Wu, J.-P.; Zhang, Y.-H.; Wang, H.-L. Numerical study on tangential velocity indicator of free vortex in the cyclone. *Sep. Purif. Technol.* 2014, *132*, pp. 541-551. http://dx.doi.org/10.1016/j.seppur.2014.06.007.

 doi:10.20944/preprints202606.0235.v1

62. Altmeyer, S.; Mathieu, V.; Jullemier, S.; Contal, P.; Midoux, N.; Rode, S.; Leclerc, J.-P. Comparison of different models of cyclone prediction performance for various operating conditions using a general software. *Chem. Eng. Process. Process Intensif.* 2004, 43, pp. 511-522. doi:10.1016/S0255-2701(03)00079-5.
63. Taiwo, M.I.; Namadi, M.A.; Mokwa, J.B. Design and analysis of cyclone dust separator. *American Journal of Engineering Research (AJER)*. 2016, 5(4), pp. 130-134. www.ajer.org.
64. Kim, J.C.; Lee, K.W. Experimental study of particle collection by small cyclones. *Aerosol. Sci. Tech.* 1990, 12(4). pp. 1003-1015. https://doi.org/10.1080/02786829008959410.
65. Wang, B.; Xu, D.L.; Chu, K.W.; Yu, A.B. Numerical study of gas-solid flow in a cyclone separator, *Appl. Math. Model*. 2006, 30(11). pp. 1326-1342. https://doi.org/10.1016/j.apm.2006.03.011.
66. Misiulia, D.; Andersson, A.G.; Lundström, T.S. Effects of the inlet angle on the flow pattern and pressure drop of a cyclone with helical-roof inlet, *Chemical Engineering Research Design*. 2015, 102, pp. 307-321. http://dx.doi.org/10.1016/j.cherd.2015.06.036.
67. Cort'es, C.; Gil, A. Modeling the gas and particle flow inside cyclone separators. *Prog. Energ. Combust*. 2007, 33(5), pp. 409-452. 10.1016/j.pecs.2007.02.001.
68. Dziubak, T. Experimental research on separation efficiency of aerosol particles in vortex tube separators with electric field, *Bull. Pol. Acad. Sci. Tech. Sci*. 2020,68(3). 503-516. 10.24425/bpasts.2020.133385.
69. Song, J.; Wei, Y.; Sun, G.; Chen, J. Experimental and CFD study of particle deposition on the outer surface of vortex finder of a cyclone separator, *Chem. Eng. J.* 2017, 309, 249-262. https://doi.org/10.1016/j.cej.2016.10.019.
70. Khazaee, I. Numerical investigation of the effect of number and shape of inlet of cyclone and particle size on particle separation, *Heat Mass Transfer*. 2017, 53(6), 2009-2016. 10.1007/s00231-016-1957-4.
71. Babaoˇglu, N.U.; Parvaz, F.; Hosseini, S.H.; Elsayed, L.; Ahmadi, G. Influence of the inlet cross-sectional shape on the performance of a multi-inlet gas cyclone, *Powder Technol*. 2021, 384, pp. 82-99. https://doi.org/10.1016/j.powtec.2021.02.008.
72. Iozia, D.L.; Leith, D. Effect of cyclone dimensions on gas flow pattern and collection efficiency, *Aerosol. Sci. Tech.* 1989, 10(3), 491-500. https://doi.org/10.1080/02786828908959289.
73. Elsayed, K.; Lacor, C. The effect of cyclone inlet dimensions on the flow pattern and performance, Appl. Math. Model. 2011, 35(4), pp. 1952-1968. https://doi.org/10.1016/j.apm.2010.11.007.
74. Zhang, J.; Zha, Z.; Che, P.; Ding, H.; Pan, W. Influences of inlet height and velocity on main performances in the cyclone separator, *Particul. Sci. Technol.* 37 (6) (2019). pp. 669–676. https://doi.org/10.1080/02726351.2018.1423589.
75. Yao, Y.; Shang, M.; Xiwei Ke ,X.; Huang, Z.; Zhou, T.; Lyu J. Effects of the inlet particle spatial distribution on the performance of a gas-solid cyclone separator. *Particuology* 2024, 85. pp. 133-145. https://doi.org/10.1016/j.partic.2023.03.024.
76. Yao, Y.; Shang, M.; Ke, X.; Zhang, J.; Zhou, T.; Lyu, J. Design of multi-stage contracted inlet duct for cyclone separators. *Sep. Purif. Technol*. 2024, 332:125753. https://doi.org/10.1016/j.seppur.2023.125753.
77. Wei, Q.; Sun, G.; Gao. C. Numerical analysis of axial gas flow in cyclone separators with different vortex finder diameters and inlet dimensions. *Powder Technol.* 2020, 369. pp. 321–333. https://doi.org/10.1016/j.powtec.2020.05.038.
78. El-Emam, M.A.; Zhou, L.; Shi, W.; Han, Ch. Performance evaluation of standard cyclone separators by using CFD–DEM simulation with realistic bio-particulate matter. *Powder Technol.* 2021, 385. pp. 357–374. https://doi.org/10.1016/j.powtec.2021.03.006.
79. Bernardo, S.; Mori, M.; Peres, A.P.; Dionısio, R.P. 3-D computational fluid dynamics for gas and gas-particle flows in a cyclone with different inlet section angles. *Powder Technol.* 2006, 162, pp. 190-200. https://doi.org/10.1016/j.powtec.2005.11.007.
80. Zhao, B.; Shen, H.; Kang, Y. Development of a symmetrical spiral inlet to improve cyclone separator performance. *Powder Technol.* 2004, 145(1). pp. 47-50. https://doi.org/10.1016/j.powtec.2004.06.001.
81. Feng, M.; Gui, Ch.; Zhou, Y.; Lei, Z. Numerical study on performance optimization and flow mechanism of a new cyclone separator. *Green Chemical Engineering* 2025, 6. pp. 76-84. https://doi.org/10.1016/j.gce.2024.03.006.

 doi:10.20944/preprints202606.0235.v1

82. Misiulia, D.; Andersson, A.G.; Lundström, T.S. Effects of the inlet angle on the collection efficiency of a cyclone with helical-roof inlet, *Powder Technol.* 2017, 305. pp. 48-55. https://doi.org/10.1016/j.powtec.2016.09.050.
83. Wang, S.; Li, H.; Wang, R.; Wang, X.; Tian, R.; Sun, Q. Effect of the inlet angle on the performance of a cyclone separator using CFD-DEM. Advanced *Powder Technol.* 2018, xxx–xxx. https://doi.org/10.1016/j.apt.2018.10.027.
84. Wasilewski, M.; Brar, L.S. Effect of the inlet duct angle on the performance of cyclone separators, *Sep. Purif. Technol*. 2019, 213, pp. 19-33. https://doi.org/10.1016/j.seppur.2018.12.023.
85. El-Emam, M.A.; Zhou, L.; Omara, A.I. Predicting the performance of aero-type cyclone separators with different spiral inlets under macroscopic bio-granular flow using CFD–DEM modelling. *Biosyst Eng*. 2023, 233. pp. 125-150. https://doi.org/10.1016/j.biosystemseng.2023.08.003.
86. Wang, Z.; Sun, G.; Song, Z.; Yuan, S.; Qian Z. Effect of inlet volute wrap angle on the flow field and performance of double inlet gas cyclones. *Particuology* 2023, 77, pp. 29-36. https://doi.org/10.1016/j.partic.2022.08.006.
87. Wasilewski, M.; Lakhbir, L.S. Performance analysis of the cyclone separator with a novel clean air inlet installed on the roof Surface. *Powder Technol.* 2023, 428, 118849. https://doi.org/10.1016/j.powtec.2023.118849.
88. Khoshraftar, Z.; Ghaemi, A. Maximizing Cyclone Efficiency: Innovating Body Rotation for Silica Particle Separation via RSM and ANNs Modeling. *Arabian Journal for Science and Engineering* 2024, 49, 8489-8507. https://doi.org/10.1007/s13369-024-08990-y.
89. Barua, S.; Batcha, M.F.M.; Mohammed, A.N.; Saif, Y.; Al-Alimi, S.; Al-fakih, M.A.M.; Zhou,W. Numerical Investigation of Inlet Height andWidth Variations on Separation Performance and Pressure Drop of Multi-Inlet Cyclone Separators. *Processes* 2024, 12, 1820. https://doi.org/10.3390/pr12091820.
90. Dong, S.; Jiang Y.; Dong, R.J.K.; Wang, B. Numerical Study of Vortex Eccentricity in Gas Cyclone. *Applied Mathematical Modelling* 2019, 80, pp. 683-701. https://doi.org/10.1016/j.apm.2019.11.024.
91. Fetuga, I.A.; Olakoyejo, O.T.; Abolarin, S.M.; Ologunoba, S.O.; Robinson, U.D; de Oliveira Siqueira A.M. Eulerian-Lagrangian fluid dynamics study on the effects of inlet radial angle on the performance and flow pattern of multi-inlet cyclone separator. *Alexandria Eng J*. 2023, 78, pp. 453-468. https://doi.org/10.1016/j.aej.2023.07.058.
92. Guo, M.; Yang, L.; Son, H.; Le, D. K.; Manickam, S.; Sun, X.; Yoon, J. Y. An Overview of Novel Geometrical Modifications and Optimizations of Gas-Particle Cyclone Separators, *Sep. Purif. Technol.* 2023, *329*, 125136. 10.1016/j.seppur.2023.125136.
93. Pandey, S.; Saha, I.; Prakash, O.; Mukherjee, T.; Iqbal, J.; Roy, A.K.; Wasilewski, M.; Brar, L.S. CFD Investigations of Cyclone Separators with Different Cone Heights and Shapes. *Appl. Sci*. 2022, 12, 4904. https://doi.org/10.3390/app12104904.
94. Zhou, C.; Dai, X.; Zhou, M.; Zeng, Y. Numerical Simulation and Influence Analysis of Geometrical Parameters in Gas–Solid Separation Process for a Cyclone Separator. *Processes* 2025, 13, 2723. https://doi.org/10.3390/pr13092723.
95. Chuah, T.G.; Gimbun, J.; Choong, T.S.Y. A CFD study of the effect of cone dimensions on sampling aerocyclones performance and hydrodynamics. *Powder Technol.* 2006; 162: pp. 126–132. https://doi.org/10.1016/j.powtec.2005.12.010.
96. Kabsch, P. Odpylanie i odpylacze. Warszawa; WNT, 1992. (in Polish).
97. Soliman, M.M.; El-shaer, Y.; Elsayed, K.; Ibrahim, M.A. Performance enhancement of gas cyclone with streamlined ports using CFD simulations. *Journal of Engineering and Applied Science* 2025, 72:4. https://doi.org/10.1186/s44147-024-00575-8.
98. Wang Z, Sun G, Jiao Y, Experimental study of large-scale single and double inlet cyclone separators with two types of vortex finder, *Chemical Engineering and Processing - Process Intensification* (2020), doi: https://doi.org/10.1016/j.cep.2020.108188
99. Jafarnezhad, A.; Salarian, H.; Kheradmand, S.; Khaleghinia, J. Performance improvement of a cyclone separator using different shapes of vortex finder under high-temperature operating conditio. Journal of the

 doi:10.20944/preprints202606.0235.v1

Brazilian *Society of Mechanical Sciences and Engineering* 2021, 43:81. https://doi.org/10.1007/s40430-020-02783-8.

100. Raoufi, A.; Shams, M.; Farzaneh, M.; Ebrahimi, R. Numerical simulation and optimization of fluid flow in cyclone vortex finder, *Chem. Eng. Process. Process Intensif.* 2008, 47(1). pp. 128–137. https://doi.org/10.1016/j.cep.2007.08.004.
101. Lim, K.S.; Kim, H.S.; Lee, K.W. Characteristics of the collection efficiency for a cyclone with different vortex finder shapes, *Journal of Aerosol Science* 2004, 35, pp. 743–754. https://doi.org/10.1016/J.JAEROSCI.2003.12.002.
102. Misiulia, D.; Andersson, A.G.; Lundström, T.S. Large Eddy Simulation investigation of an industrial cyclone separator fitted with a pressure recovery deswirler, *Chem. Eng. Technol.* 2017, 40, No. 4, pp. 709–718. DOI: 10.1002/ceat.201600505.
103. Misiulia D., Antonyuk S., Andersson A.G., Lundström T.S., Effects of deswirler position and its centre body shape as well as vortex finder extension downstream on cyclone performance, *Powder Technol*. 336 (2018) 45–56, https://doi.org/ 10.1016/j.powtec.2018.05.034.
104. Misiulia, D.; Elsayed, K.; Andersson, A.G. Geometry optimization of a deswirler for cyclone separator in terms of pressure drop using CFD and artificial neural network. *Sep. Purif. Technol*. 2017, 185, pp. 10–23. https://doi.org/10.1016/j.seppur.2017.05.025.
105. Gao, Z.; Wei, Y.; Liu, Z.; Jia, C.; Wang, J.; Wang, J.; Mao, Y. Internal Components Optimization in Cyclone Separators: Systematic Classification and Meta-analysis. *Sep. Purif. Rev.* 2021, 50, 4. 400-416. DOI: 10.1080/15422119.2020.1789995.
106. Zhou, F.; Sun, G.; Han, X.; Zhang, Y.; Bi, W. Experimental and CFD Study on Effects of Spiral Guide Vanes on Cyclone Performance. *Adv. Powder Technol*. 2018, 29, 3394–3403. DOI:10.1016/j.apt.2018.09.022.
107. Misyulya, D.I. New Designs of Devices for a Decrease in Power Consumption of Cyclone Dust Collectors. *Russian Journal of Non Ferrous Metals*, 2012, 53(1), pp. 57-61.
108. Xu, W.; Li, Q.; Wang, J.; Jin, Y. Performance evaluation of a new cyclone separator – Part II simulation results, *Sep. Purif. Technol*. 2016, 160, pp. 112-116, https://doi.org/10.1016/j.seppur.2016.01.012.
109. Fu, S.; Zhou,F.; Sun, G.; Yuan, H.; Zhu J. Performance evaluation of industrial large-scale cyclone separator with novel vortex Finder. *Adv. Powder Technol.* 32 (2021) 931–939. https://doi.org/10.1016/j.apt.2021.01.033.
110. Sun, Y.H.; Yang, G.G.; Shen, Q., Li S.; Yang, X.; Zhang, G.; Sheng, Z. Numerical analysis of cyclone separators with unique Dipleg structures at different Dipleg-to-dustbin ratios. *Powder Technol.* 2024, 443, 119904. https://doi.org/10.1016/j.powtec.2024.119904.
111. Elsayed, K.; Parvaz, F.; Hosseini, S.H.; Ahmadie, G. Influence of the dipleg and dustbin dimensions on performance of gas cyclones: An optimization study. *Sep. Purif. Technol*. 2020, 239, 116553, https://doi.org/10.1016/j.seppur.2020.116553.
112. Parvaz, F.; Hosseini, S.H.; Elsayed, K.; Ahmadi, G. Influence of the Dipleg Shape on the Performance of Gas Cyclones. *Sep. Purif. Technol*. 2020, 233, 116000. https://doi.org/10.1016/j.seppur.2019.116000.
113. Kaya, F.; Karagoz, I. Numerical investigation of performance characteristics of a cyclone prolonged with a dipleg, *Chemical Engineering Journal*. 2009, 151, pp. 39-45. https://doi.org/10.1016/j.cej.2009.01.040.
114. Wasilewski, M. Analysis of the effect of counter-cone location on cyclone separator efficiency *Sep. Purif. Technol*. 2017, 179, pp. 236-247. https://doi.org/10.1016/j.seppur.2017.02.012.
115. Yoshida, H. Effect of apex cone shape and local fluid flow control method on fine particle classification of gas-cyclone, *Chem. Eng. Sci.* 2013, 85, pp. 55-58. https://doi.org/10.1016/j.ces.2012.01.060.
116. Yoshida, H.; Nishimura, Y.; Fukui, K.; Yamamoto, T. Effect of apex cone shape on fine particle classification of gas-cyclone, *Powder Technol*. 2010, 204, pp. 54-62. https://doi.org/10.1016/j.powtec.2010.07.006.
117. Huang, L.; Deng, S.; Chen, Z.; Guan, J.; Chen, M. Numerical analysis of a novel gas-liquid pre-separation cyclone. *Sep. Purif. Technol*. 2018, 194, pp. 470-479. https://doi.org/10.1016/j.seppur.2017.11.066.
118. Jo, Y.; Tien, Ch.; Ray, M.B. Development of a post cyclone to improve the efficiency of reverse flow cyclones. *Powder Technol.* 2000, 113, No 1-2: pp. 97-108. https://doi.org/10.1016/S0032-5910(00)00206-0.
119. Jung, Ch.H.; Xiang, R.B.; Kim, M.C.; Lim, K.S.; Lee, K.W. Performance evaluation of a cyclone with granular packed beds. *J. Aerosol Sci.* 2004, 35, No 12: pp. 1483-1496. https://doi.org/10.1016/j.jaerosci.2004.06.076.

 doi:10.20944/preprints202606.0235.v1

120. Wasilewski, M.; Ligus, G.; L.S. Investigations of the flow phenomena inside square cyclone separators with different prismatic heights. *Sep. Purif. Technol* 2025, 362, 131724. https://doi.org/10.1016/j.seppur.2025.131724.
121. Chlebnikovas, A.; Paliulis, D.; Kilikevičiene, K.; Kilikevičius, A. Experimental Research of Gaseous Emissions Impact on the Performance of New-Design Cylindrical Multi-Channel Cyclone with Adjustable Half-Rings. *Sustainability* 2022, 14, 902. https://doi.org/10.3390/su14020902.
122. Yao, Y.; Huang, Z.; Zhou, T.; Li, J.; Cheng, L.; Zhang, M.; Yang, H.; Lyu, J. Double-Eccentric Design for the Vortex Finder of a Cyclone Separator. *Ind. Eng. Chem. Res.* 2022, 61, 14927−14939. https://doi.org/10.1021/acs.iecr.2c02054.
123. Kim, H.T.; Zhu, Y.; Hinds, W.C.; Lee, K.W. Experimental study of small virtual cyclones as particle concentrators, *J. Aerosol Sci*. 2002, 33(5). pp. 721-733, https://doi.org/ 10.1016/S0021-8502(01)00212-9.
124. Dziubak, T. The problems of dust extraction from air intake cyclonic dedusters of special vehicle engines, *Combust. Engines* 2009, 4(139). pp. 34-44 (In Polish). https://doi.org/10.19206/CE-117166.
125. PN-ISO 5011, 1994. Filtry powietrza do silników spalinowych i sprężarek. Badanie działania, Polski Komitet Normalizacyjny, 1994.
126. Dziubak, T. Experimental Dust Absorption Study in Automotive Engine Inlet Air Filter. *Materials*. 2024, 17, 3249. https:// doi.org/10.3390/ma17133249.
127. Wang J., Kim S.C., Pui D.Y.H.: Figure of Merit of Composite Filters with Micrometer and Nanometer Fibers. *Aerosol. Sci.Tech.* 2008, 42, pp. 722-728. 10.1080/02786820802249133.
128. Zhang, Y.; Yang, S.; Hu, J.; Wang H. Impact of draft plate on the separation performance of gas-solid cyclone separator. *Powder Technol*. 2025, 456, 120806. https://doi.org/10.1016/j.powtec.2025.120806.
129. Zhang, S.; Shin, W.G. The effect of a counter cone on the performance of an axial cyclone separator. *J. Mech. Sci. Techno.* 2023, 37(9), pp. 4889-4898. http://doi.org/10.1007/s12206-023-0842-6.
130. Ramachandran, O.; Raynor, P.C.; Leith, D. Collection efficiency and pressure drop for a rotary-flow cyclone. *Filtr. Sep.* 1994, 31, pp. 631-636. https://doi.org/10.1016/0015-1882(94)80070-7.
131. Li, J.; Cai, W. Study of the cut diameter of solid–gas separation in cyclone with electrostatic excitation. *Journal of Electrostatics* 2004, 60, pp. 15-23. 10.1016/j.elstat.2003.05.001.